ANL-ZPR-473

ANL-ZPR-473

APPLIED PHYSICS DIVISION
APPLIED PHYSICS DIVISION
APPLIED PHYSICS DIVISION
APPLIED PHYSICS DIVISION
APPLIED PHYSICS DIVISION
APPLIED PHYSICS DIVISION
APPLIED PHYSICS DIVISION
APPLIED PHYSICS DIVISION
APPLIED PHYSICS DIVISION
APPLIED PHYSICS DIVISION
APPLIED PHYSICS DIVISION
APPLIED PHYSICS DIVISION
APPLIED PHYSICS DIVISION
APPLIED PHYSICS DIVISION
APPLIED PHYSICS DIVISION
APPLIED PHYSICS DIVISION
APPLIED PHYSICS DIVISION
APPLIED PHYSICS DIVISION

ZPPR Progress Report: January 1987 through March 1987

Argonne National Laboratory–West, Idaho Falls, Idaho 83403-2528
Operated by the University of Chicago
for the United States Department of Energy Under Contract W-31-109-Eng-38

APPLIED PHYSICS DIVISION
APPLIED PHYSICS DIVISION
APPLIED PHYSICS DIVISION
APPLIED PHYSICS DIVISION
APPLIED PHYSICS DIVISION

CONTENTS:

•ZPPR-15D Sodium Void
•ZPPR-15D Control Rods
•ZPPR-15D Reaction Rates
•ZPPR-15C and 15D Models
•ZPPR-15D Noise Coherence
•ZPPR-15B and 15D Gamma Dose

Issued April 27, 1987

Argonne National Laboratory, with facilities in the states of Illinois and Idaho, is owned by the United States government, and operated by The University of Chicago under the provisions of a contract with the Department of Energy.

DISCLAIMER

ANL-ZPR--473

TI87 028067

ZPPR PROGRESS REPORT: JANUARY 1987 THROUGH MARCH 1987

edited by

S. B. Brumbach and P. J. Collins

Applied Physics Division
Argonne National Laboratory - West
P.O. Box 2528
Idaho Falls, ID 83403-2528

[redacted]

~~Any further distribution by~~ any ho~~lder of this document or o~~f the ~~data therein to third pa~~rties re~~presenting foreign intere~~sts, ~~foreign governments,~~ foreig~~n companies and fo~~reign ~~subsidiaries or foreign d~~ivisions ~~of U.S. companies should~~ be ~~coordinated with the D~~eputy Ass~~istant Secretary for Rea~~ctor ~~Systems Development~~ Techno~~logy, U.S. Department~~ of [redacted]

April 27, 1987

DISCLAIMER

TABLE OF CONTENTS

		Page
1.	**PROGRAM STATUS** (S. B. Brumbach and P. J. Collins).....	1
2.	**CALCULATION MODELS FOR ZPPR-15C** (G. L. Grasseschi and P. J. Collins)	4
3.	**MULTIGROUP CROSS SECTION DATA AND CALCULATION MODELS FOR ZPPR-15D** (G. L. Grasseschi and P. J. Collins).....	19
4.	**CALCULATED K-EFFECTIVE AND DELAYED NEUTRON PARAMETERS FOR ZPPR-15C and ZPPR-15D** (G. L. Grasseschi and P. J. Collins).....	28
5.	**MEASUREMENTS AND ANALYSIS OF REACTION RATES IN ZPPR-15D** (P. J. Collins, J. M. Gasidlo, G. L. Grasseschi and D. W. Maddison).....	32
6.	**BASIC DATA FOR REACTION RATE MEASUREMENTS IN ZPPR-15D** (D. W. Maddison and J. M. Gasidlo).....	56
7.	**IN-CELL REACTION RATE MEASUREMENTS AND CELL FACTORS FOR ZPPR ASSEMBLY 15D** (J. M. Gasidlo and D. W. Maddison).....	62
8.	**MEASUREMENT AND ANALYSIS OF CONTROL ROD WORTHS IN ZPPR-15D** (D. M. Smith and P. J. Collins).....	68
9.	**SODIUM VOID MEASUREMENTS AND ANALYSIS IN ZPPR-15D** (S. B. Brumbach, R. E. Kaiser and G. L. Grasseschi).....	77
10.	**GAMMA RAY DOSE DISTRIBUTION IN THE ZPPR-15B CORE AND SHIELDING EXPERIMENTS** (D. N. Olsen and T. S. Huntsman).....	83
11.	**GAMMA RAY DOSE DISTRIBUTION IN ZPPR-15D** (D. N. Olsen and T. S. Huntsman).....	90
12.	**NOISE COHERENCE MEASUREMENTS IN ZPPR-15D** (S. G. Carpenter and R. W. Goin).....	95
13.	**COMPUTER PROGRAM TO PRODUCE ASSEMBLY DESCRIPTIONS FOR DETERMINISTIC CALCULATIONS** (R. W. Schaefer and D. A. Tate).....	100

ZPPR PROGRESS REPORT: JANUARY 1987 THROUGH MARCH 1987

edited by

S. B. Brumbach and P. J. Collins

ABSTRACT

Results are presented for the ZPPR-15B, 15C and 15D assemblies. These assemblies were part of the IFR Physics Test Program to provide modern integral physics data for metallic-fuelled LMRs. The ZPPR-15B assembly had a ternary fuel alloy of plutonium, depleted uranium and zirconium. In ZPPR-15C, about half of the fuel elements were converted to ^{235}U fuel, while in ZPPR-15D about 90% of the fuel was ^{235}U. Results from ZPPR-15D include foil reaction rates, control rod worths, sodium void worths, gamma ray dose distributions and noise coherence measurements. Multigroup cross section data processing and calculation models are presented for the assemblies containing ^{235}U fuel.

1. ZPPR PROGRAM STATUS (S. B. Brumbach, P. J. Collins and R. W. Schaefer)

The period January through March saw the beginning of the JUPITER-III program, a cooperative effort between the U.S. DOE and PNC of Japan. The first assembly in the program is ZPPR-17, an axially heterogeneous benchmark of about 700 MWe size. The intitial configuration, designated ZPPR-17A, is a physics benchmark with no control rods or control rod positions. Initial criticality for ZPPR-17A was on February 23, 1987.

Experiments completed so far in ZPPR-17A are operational measurements, control rod worths and sodium void worths. Control rod measurements focused on worths of a single, central rod as a function of size, composition and geometry. Sodium void measurements were made with a plate substitution technique in a zone just outside the inner core (the inner core contains the internal axial blanket) and in a zone at the core center. In addition, an oscillator technique was used to measure the sodium void worth in a single drawer in ten radial locations. A new device called the self-contained oscillator drawer was used. This device allows axial sample oscillation within a drawer at essentially any matrix location.

Analysis of most of the ZPPR-15D experiments has been completed. The results for criticality, reaction rates, sodium void and control rod worths are included in this report. The measurements and analysis of Doppler reactivity in 15B and 15D remain to be reported. The new gamma-heating capability in the ARC system has recently become available and it is intended to do analysis of ZPPR-15 measurements this summer; experimental data are given in this report. Analysis of sodium void and reaction rates in the 50% Pu fuelled/50% U fuelled core, ZPPR-15C, is continuing. Other measurements in ZPPR-15 which are not yet analyzed or reported include the high-Zr zone in 15B, helium production in a control rod in 15D and small sample worths in both 15B and 15D. The initial analysis of spectrum measurements in 15B and 15D showed problems in the data reduction. These data are currently being reanalyzed and measurements reported for ZPPR-15A will be revised.

Data processing and analysis for ZPPR-16 is continuing. The initial results show errors of 5-10% in calculated reaction rates at the edge of the core approaching the BeO reflector. Experimental control rod worths in ZPPR-16A have been obtained to good accuracy. However, data reduction for reflector worths has proven less tractable because of difficulties in calculating reliable detector efficiencies and effective source worths. Refinements in the analysis are being sought.

A study has been made of analysis issues related to ZPPR-16C. This assembly had a number of features that place special demands on analysis methods and models. Among these features are 1) the presence of polyethylene in the coolant channels, 2) high leakage and small core volume, and 3) a thick, very low density region between the core and an effective radial reflector (room return shield). Computational accuracy and limitations were explored using model problems. It was found that conventional ZPPR cross section processing methods are reasonably accurate, despite the presence of polyethylene. Large errors were encountered when the boron carbide control rods were not modeled adequately. Fortunately, these errors can be made small without a large effort. The presence of very low density regions between the core and an effective reflector leads to significant errors in nodal transport solutions. This limitation is more bothersome because this is the only deterministic transport theory method available at ZPPR that handles three explicit dimensions. Although the study focused exclusively on ZPPR-16C, many of the observations have broader implications. The study is described in detail in the report ANL-ZPR-474.

A computer program (NIPPER) has been developed to create analytical models in ARC system format directly from the ZPPR loading records. The user supplies only an overall description of the model required (zone descriptions, isotope names, etc.) and the geometry and composition input is created automatically. Complex models can now be set up simply and reliably. This system is described in Section 13 of this report. The NIPPER code has been used to construct the reference model for ZPPR-17A using xyz geometry with detailed compositions for each drawer master for

five axial slices. The model has been checked in detail against the experimental masses for all materials.

2. CALCULATION MODELS FOR ZPPR-15C (G. L. Grasseschi and P. J. Collins)

The ZPPR-15C assembly had approximately half of the drawers loaded with ^{235}U fuel (872 kg ^{235}U) and half loaded with plutonium fuel (569 kg ^{239}Pu). The loading is given in ZPR-TM-471, p. 3 et seq. Cross sections were not processed specifically for ZPPR-15C. Those for the plutonium drawers were taken from the ZPPR-15B library (ZPR-TM-470, p. 13) and those for the uranium-fuelled drawers were taken from the ZPPR-15D library, described in Section 3.

The drawer masters used in ZPPR-15C are listed in Table 2.1 and the homogenized atomic densities for the new drawers introduced are given in Table 2.2. Compositions for the plutonium drawers are given in ZPR-TM-470.

The reference calculation model for ZPPR-15C was a one-eigth core xyz representation (upper right hand quadrant of half-one). Individual master compositions were represented with the exception of fission chamber and thermocouple drawers which, unlike the basic drawers, were not symmetrically loaded in the assembly. Figure 2.1 shows the one-quarter xy midplane map with the individual drawer masters identified by matrix position.

A complication in the 15C model arises because each uranium fuel piece is 2.8 mm (0.11 in.) longer than its plutonium fuel counterpart. Since each drawer master is made up with three fuel pieces in a fuel column, the total fuel height in a uranium-fuelled drawer is 466.34 mm (18.36 in.) compared with 457.96 (18.03 in.) for the plutonium-fuelled drawers. To permit different options in modelling the assembly, compositions for the uranium drawers were derived for an axial region, 18.03 in. to 18.36 in., in addition to the regions used for ZPPR-15B (0 to 18.03 in.). These compositions are given in Table 2.2 Note that axial blanket compsitions for uranium-fuelled drawers were different from those for plutonium drawers. The axial regions in Table 2.2 are labelled by the nearest inch for brevity and 18* is used to represent 18.36 inches. Minor

isotopes, at the bottom of the table starting with phosphorus, were omitted in the calculations.

It is desirable in nodal diffusion calculations and necessary in nodal transport calculations to use a relatively coarse axial node spacing. In the reference xyz model, the core height was chosen to be the height of the uranium fuel. Axial node boundaries, given in inches for simplicity, were chosen to be 6.03 in., 12.03., 16.03., and 18.36 in. in the core, and at 24.03 in., 31.03 in., 36.15. and 42.03 in. in the axial blanket and axial reflectors. The upper node in the core used a mixture of atom densities including both core and axial blanket materials. Materials between 16.03 in and 18.03 in. had a weighting factor of 0.8584 and the materials between 18.03 in. and 18.36 in. had a weighting factor of 0.1416. This was intended to preserve atomic densities in regions of highest importance near the midplane, with the smeared material in regions of lower importance near the top of the core.

The calculated k_{eff} values are compared with those for ZPPR-15D in Section 4.

TABLE 2.1. Drawer Masters for ZPPR-15C

Zone	Drawer Master	Description
Inner Core (central 148 drawers)	138	Fuel - SC Pu - Symmetric Zr
	139	Fuel - SC Pu - Symmetric Zr
	140	Fuel - SC Pu - Symmetric Zr
	901	Fuel - SC 1/16 U - Symmetric Zr
	902	Fuel - SC 1/16 U - Symmetric Zr
	903	Fuel - SC 1/16 U - Symmetric Zr
	713	Fuel - SC Pu - Symmetric Zr - FC
	735	Fuel - SC 1/16 U - Symmetric Zr - FC
	827,828	Fuel - SC Pu - Symmetric Zr - PSR
Inner Core	141,142	Fuel - SC Pu - Asymmetric Zr
	143,144	Fuel - SC Pu - Asymmetric Zr
	145,146	Fuel - SC Pu - Asymmetric Zr
	149,150	Fuel - SC Pu - Asymmetric Zr
	905,906	Fuel - SC 1/16 U - Asymmetric Zr
	907,908	Fuel - SC 1/16 U - Asymmetric Zr
	909,910	Fuel - SC 1/16 U - Asymmetric Zr
	911,912	Fuel - SC 1/16 U - Asymmetric Zr
	913,914	Fuel - SC 1/16 U - Asymmetric Zr
	915,916	Fuel - SC 1/8 U - Asymmetric Zr
	917,918	Fuel - SC 1/8 U - Asymmetric Zr
	919,920	Fuel - SC 1/8 U - Asymmetric Zr
	929,930	Fuel - SC 1/8 U - Asymmetric Zr
	714	Fuel - SC Pu - Asymmetric Zr -FC
	736,737	Fuel - SC 1/16 U - Asymmetric Zr - FC
	738	Fuel - SC 1/8 U - Asymmetric Zr - FC

TABLE 2.1. **(contd)**

Zone	Drawer Master	Description
Outer Core	105	Fuel - SC Pu
	201	Fuel - DC Pu
	203	Fuel - DC Pu
	921,922	Fuel - SC 1/16 U - Asymmetric DU
	923	Fuel - SC 1/8 U
	924	Fuel - SC 1/8 U
	925	Fuel - DC 1/16 U
	926	Fuel - DC 1/16 U
	927	Fuel - DC 1/16 U
	928	Fuel - SC 1/8 U
	702	Fuel - SC Pu - FC
	703	Fuel - DC Pu - FC
	707	Fuel - DC Pu - Thermocouple
	741	Fuel - DC 1/16 - FC
	803,804	Fuel - SC Pu - PSR
Radial Blanket	501	DU
	704	DU - FC
Radial Reflector	401	Stainless Steel
	402	Stainless Steel
	403	Stainless Steel
	404	Stainless Steel
	405	Stainless Steel
	406	Stainless Steel
	705	Stainless Steel - FC

SC - single fuel column
Pu - ZPPR Pu/U/Mo fuel
DC - double fuel column
U - 93% enriched uranium fuel
DU - depleted uranium metal
FC - fission chamber
PSR - a narrow drawer adjacent to a poison safety rod or shim rod

TABLE 2.2. ZPPR Assembly 15C -- Atom Densities (atoms/barn-cm)

	Master 901			Master 902		
Isotopes[a]	0-18	18-18*	18-31	0-18	18-18*	18-31
C	0.0000796	0.0000342	0.0000515	0.0000839	0.0000342	0.0000515
O	0.0000006	0.0000006	0.0000007	0.0000006	0.0000006	0.0000007
Na	0.0083220	0.0093249	0.0093062	0.0083220	0.0093249	0.0093062
Si	0.0003554	0.0001490	0.0001887	0.0004330	0.0001490	0.0001887
Al	0.0000049	0.0000028	0.0000028	0.0000049	0.0000028	0.0000028
Mn	0.0004966	0.0002116	0.0003341	0.0005069	0.0002116	0.0003341
Cr	0.0054659	0.0024724	0.0040597	0.0055400	0.0024724	0.0040597
Fe	0.0193365	0.0088343	0.0144338	0.0191887	0.0088343	0.0144338
Ni	0.0024216	0.0010619	0.0017164	0.0024188	0.0010619	0.0017164
Cu	0.0000302	0.0000281	0.0000423	0.0000302	0.0000281	0.0000423
Zr	0.0020955	---	---	0.0020955	---	---
Mo	0.0000138	0.0000135	0.0000330	0.0000138	0.0000135	0.0000330
U234	0.0000109	0.0000109	---	0.0000109	0.0000109	---
U235	0.0011296	0.0011480	0.0000326	0.0011296	0.0011480	0.0000326
U236	0.0000052	0.0000053	---	0.0000052	0.0000053	---
U238	0.0073391	0.0145894	0.0145301	0.0073386	0.0145894	0.0145302
P	0.0000158	0.0000055	0.0000100	0.0000161	0.0000055	0.0000100
S	0.0000049	0.0000011	0.0000079	0.0000084	0.0000011	0.0000079
Cl	0.0000003	0.0000003	0.0000003	0.0000003	0.0000003	0.0000003
Ca	0.0000019	0.0000021	0.0000021	0.0000019	0.0000021	0.0000021
Co	0.0000017	0.0000011	0.0000008	0.0000017	0.0000011	0.0000008
LIP	0.0000028	0.0000016	0.0000016	0.0000028	0.0000016	0.0000016
HIP	0.0000018	0.0000011	0.0000011	0.0000018	0.0000011	0.0000011

TABLE 2.2. (contd)

	Master 903			Master 905 and 906		
Isotopes[a]	0-18	18-18*	18-31	0-18	18-18*	18-31
C	0.0000839	0.0000342	0.0000515	0.0000817	0.0000342	0.0000515
O	0.0000006	0.0000006	0.0000007	0.0000006	0.0000006	0.0000007
Na	0.0083220	0.0093249	0.0093062	0.0083220	0.0093249	0.0093062
Si	0.0004330	0.0001490	0.0001887	0.0002268	0.0001490	0.0001887
Al	0.0000049	0.0000028	0.0000028	0.0000049	0.0000028	0.0000028
Mn	0.0005069	0.0002116	0.0003341	0.0004467	0.0002116	0.0003341
Cr	0.0055400	0.0024724	0.0040597	0.0054356	0.0024724	0.0040597
Fe	0.0191887	0.0088343	0.0144338	0.0194049	0.0088343	0.0144338
Ni	0.0024188	0.0010619	0.0017164	0.0023237	0.0010619	0.0017164
Cu	0.0000302	0.0000281	0.0000423	0.0000534	0.0000281	0.0000423
Zr	0.0021073	---	---	0.0022117	---	---
Mo	0.0000138	0.0000135	0.0000330	0.0000324	0.0000135	0.0000330
U234	0.0000109	0.0000109	---	0.0000109	0.0000109	---
U235	0.0011297	0.0011480	0.0000326	0.0011298	0.0011480	0.0000326
U236	0.0000052	0.0000053	---	0.0000052	0.0000053	---
U238	0.0073498	0.0145894	0.0145302	0.0073385	0.0145894	0.0145302
P	0.0000161	0.0000055	0.0000100	0.0000118	0.0000055	0.0000100
S	0.0000084	0.0000011	0.0000079	0.0000015	0.0000011	0.0000079
Cl	0.0000003	0.0000003	0.0000003	0.0000003	0.0000003	0.0000003
Ca	0.0000019	0.0000021	0.0000021	0.0000019	0.0000021	0.0000021
Co	0.0000017	0.0000011	0.0000008	0.0000017	0.0000011	0.0000008
LIP	0.0000028	0.0000016	0.0000016	0.0000028	0.0000016	0.0000016
HIP	0.0000018	0.0000011	0.0000011	0.0000018	0.0000011	0.0000011

TABLE 2.2. (contd)

	Master 907 and 908			Master 909 and 910		
Isotopes[a]	0-18	18-18*	18-31	0-18	18-18*	18-31
C	0.0000817	0.0000342	0.0000515	0.0000710	0.0000342	0.0000515
O	0.0000006	0.0000006	0.0000007	0.0000006	0.0000006	0.0000007
Na	0.0083220	0.0093249	0.0093062	0.0083220	0.0093249	0.0093062
Si	0.0002268	0.0001490	0.0001887	0.0002379	0.0001490	0.0001887
Al	0.0000049	0.0000028	0.0000028	0.0000049	0.0000028	0.0000028
Mn	0.0004467	0.0002116	0.0003341	0.0004422	0.0002116	0.0003341
Cr	0.0054356	0.0024724	0.0040597	0.0054421	0.0024724	0.0040597
Fe	0.0194049	0.0088343	0.0144338	0.0193354	0.0088343	0.0144338
Ni	0.0023237	0.0010619	0.0017164	0.0023279	0.0010619	0.0017164
Cu	0.0000534	0.0000281	0.0000423	0.0000530	0.0000281	0.0000423
Zr	0.0022151	---	---	0.0021391	---	---
Mo	0.0000324	0.0000135	0.0000330	0.0000409	0.0000135	0.0000330
U234	0.0000109	0.0000109	---	0.0000109	0.0000109	---
U235	0.0011298	0.0011480	0.0000326	0.0011298	0.0011480	0.0000326
U236	0.0000052	0.0000053	---	0.0000052	0.0000053	---
U238	0.0073385	0.0145894	0.0145302	0.0073345	0.0145894	0.0145302
P	0.0000118	0.0000055	0.0000100	0.0000126	0.0000055	0.0000100
S	0.0000015	0.0000011	0.0000079	0.0000073	0.0000011	0.0000079
Cl	0.0000003	0.0000003	0.0000003	0.0000003	0.0000003	0.0000003
Ca	0.0000019	0.0000021	0.0000021	0.0000019	0.0000021	0.0000021
Co	0.0000017	0.0000011	0.0000008	0.0000017	0.0000011	0.0000008
LIP	0.0000028	0.0000016	0.0000016	0.0000028	0.0000016	0.0000016
HIP	0.0000018	0.0000011	0.0000011	0.0000018	0.0000011	0.0000011

TABLE 2.2. **(contd)**

	Master 911 and 912			Master 913 and 914		
Isotopes[a]	0-18	18-18*	18-31	0-18	18-18*	18-31
C	0.0000710	0.0000342	0.0000515	0.0000710	0.0000342	0.0000515
O	0.0000006	0.0000006	0.0000007	0.0000006	0.0000006	0.0000007
Na	0.0083220	0.0093249	0.0093062	0.0083220	0.0093249	0.0093062
Si	0.0002379	0.0001490	0.0001887	0.0002379	0.0001490	0.0001887
Al	0.0000049	0.0000028	0.0000028	0.0000049	0.0000028	0.0000028
Mn	0.0004422	0.0002116	0.0003341	0.0004422	0.0002116	0.0003341
Cr	0.0054421	0.0024724	0.0040597	0.0054421	0.0024724	0.0040597
Fe	0.0193354	0.0088343	0.0144338	0.0193354	0.0088343	0.0144338
Ni	0.0023279	0.0010619	0.0017164	0.0023279	0.0010619	0.0017164
Cu	0.0000530	0.0000281	0.0000423	0.0000530	0.0000281	0.0000423
Zr	0.0021549	---	---	0.0022079	---	---
Mo	0.0000409	0.0000135	0.0000330	0.0000409	0.0000135	0.0000330
U234	0.0000109	0.0000109	---	0.0000109	0.0000109	---
U235	0.0011298	0.0011480	0.0000326	0.0011298	0.0011480	0.0000326
U236	0.0000052	0.0000053	---	0.0000052	0.0000053	---
U238	0.0073345	0.0145894	0.0145302	0.0073345	0.0145894	0.0145302
P	0.0000126	0.0000055	0.0000100	0.0000126	0.0000055	0.0000100
S	0.0000073	0.0000011	0.0000079	0.0000073	0.0000011	0.0000079
Cl	0.0000003	0.0000003	0.0000003	0.0000003	0.0000003	0.0000003
Ca	0.0000019	0.0000021	0.0000021	0.0000019	0.0000021	0.0000021
Co	0.0000017	0.0000011	0.0000008	0.0000017	0.0000011	0.0000008
LIP	0.0000028	0.0000016	0.0000016	0.0000028	0.0000016	0.0000016
HIP	0.0000018	0.0000011	0.0000011	0.0000018	0.0000011	0.0000011

TABLE 2.2. **(contd)**

	Master 915 and 916			Master 917 and 918		
Isotopes[a]	0-18	18-18*	18-31	0-18	18-18*	18-31
C	0.0000817	0.0000342	0.0000515	0.0000817	0.0000342	0.0000515
O	0.0000006	0.0000006	0.0000007	0.0000006	0.0000006	0.0000007
Na	0.0083220	0.0093249	0.0093062	0.0083220	0.0093249	0.0093062
Si	0.0002271	0.0001493	0.0001887	0.0002271	0.0001493	0.0001887
Al	0.0000049	0.0000028	0.0000028	0.0000049	0.0000028	0.0000028
Mn	0.0004467	0.0002116	0.0003341	0.0004467	0.0002116	0.0003341
Cr	0.0054386	0.0024754	0.0040597	0.0054386	0.0024754	0.0040597
Fe	0.0194151	0.0088445	0.0144338	0.0194151	0.0088445	0.0144338
Ni	0.0023259	0.0010641	0.0017164	0.0023259	0.0010641	0.0017164
Cu	0.0000534	0.0000281	0.0000423	0.0000534	0.0000281	0.0000423
Zr	0.0022117	---	---	0.0022151	---	---
Mo	0.0000326	0.0000137	0.0000330	0.0000326	0.0000137	0.0000330
U234	0.0000218	0.0000218	---	0.0000218	0.0000218	---
U235	0.0022380	0.0022581	0.0000326	0.0022380	0.0022581	0.0000326
U236	0.0000104	0.0000104	---	0.0000104	0.0000104	---
U238	0.0074092	0.0146518	0.0145302	0.0074054	0.0146518	0.0145302
P	0.0000118	0.0000055	0.0000100	0.0000118	0.0000055	0.0000100
S	0.0000015	0.0000011	0.0000079	0.0000015	0.0000011	0.0000079
Cl	0.0000003	0.0000003	0.0000003	0.0000003	0.0000003	0.0000003
Ca	0.0000019	0.0000021	0.0000021	0.0000019	0.0000021	0.0000021
Co	0.0000017	0.0000011	0.0000008	0.0000017	0.0000011	0.0000008
LIP	0.0000028	0.0000016	0.0000016	0.0000028	0.0000016	0.0000016
HIP	0.0000018	0.0000011	0.0000011	0.0000018	0.0000011	0.0000011

TABLE 2.2. **(contd)**

	Master 919 and 920			Master 921 and 922		
Isotopes[a]	0-18	18-18*	18-31	0-18	18-18*	18-31
C	0.0000710	0.0000342	0.0000515	0.0000781	0.0000341	0.0000515
O	0.0000006	0.0000006	0.0000007	0.0000006	0.0000007	0.0000007
Na	0.0083220	0.0093249	0.0093062	0.0083220	0.0093249	0.0093062
Si	0.0002381	0.0001497	0.0001887	0.0002699	0.0001547	0.0001887
Al	0.0000049	0.0000028	0.0000028	0.0000049	0.0000028	0.0000028
Mn	0.0004421	0.0002116	0.0003341	0.0005123	0.0002111	0.0003341
Cr	0.0054442	0.0024798	0.0040597	0.0063823	0.0024693	0.0040597
Fe	0.0193428	0.0088597	0.0144338	0.0226061	0.0088229	0.0144338
Ni	0.0023298	0.0010672	0.0017164	0.0027164	0.0010615	0.0017164
Cu	0.0000530	0.0000281	0.0000423	0.0000608	0.0000281	0.0000423
Zr	0.0021391	---	---	0.0000001	---	---
Mo	0.0000411	0.0000141	0.0000330	0.0000565	0.0000138	0.0000330
U234	0.0000214	0.0000211	---	0.0000109	0.0000108	---
U235	0.0022041	0.0021871	0.0000326	0.0011256	0.0011311	0.0000326
U236	0.0000103	0.0000101	---	0.0000052	0.0000052	---
U238	0.0074145	0.0146475	0.0145302	0.0073188	0.0145884	0.0145302
P	0.0000126	0.0000056	0.0000100	0.0000158	0.0000055	0.0000100
S	0.0000073	0.0000012	0.0000079	0.0000137	0.0000011	0.0000079
Cl	0.0000003	0.0000003	0.0000003	0.0000003	0.0000003	0.0000003
Ca	0.0000019	0.0000021	0.0000021	0.0000019	0.0000021	0.0000021
Co	0.0000017	0.0000011	0.0000008	0.0000016	0.0000011	0.0000008
LIP	0.0000028	0.0000016	0.0000016	0.0000028	0.0000016	0.0000016
HIP	0.0000018	0.0000011	0.0000011	0.0000018	0.0000011	0.0000011

TABLE 2.2. **(contd)**

	Master 923			Master 924		
Isotopes[a]	0-18	18-18*	18-31	0-18	18-18*	18-31
C	0.0000782	0.0000342	0.0000515	0.0000781	0.0000342	0.0000515
O	0.0000006	0.0000006	0.0000007	0.0000006	0.0000006	0.0000007
Na	0.0083220	0.0093249	0.0093062	0.0083220	0.0093249	0.0093062
Si	0.0002691	0.0001497	0.0001887	0.0002691	0.0001497	0.0001887
Al	0.0000049	0.0000028	0.0000028	0.0000049	0.0000028	0.0000028
Mn	0.0005125	0.0002116	0.0003341	0.0005125	0.0002116	0.0003341
Cr	0.0063876	0.0024798	0.0040597	0.0063876	0.0024798	0.0040597
Fe	0.0226246	0.0088597	0.0144338	0.0226246	0.0088594	0.0144338
Ni	0.0027195	0.0010672	0.0017164	0.0027195	0.0010671	0.0017164
Cu	0.0000608	0.0000281	0.0000423	0.0000608	0.0000281	0.0000423
Zr	0.0000001	---	---	0.0000001	---	---
Mo	0.0000567	0.0000141	0.0000330	0.0000567	0.0000141	0.0000330
U234	0.0000214	0.0000211	---	0.0000214	0.0000211	---
U235	0.0022041	0.0021871	0.0000326	0.0022043	0.0021871	0.0000326
U236	0.0000103	0.0000101	---	0.0000103	0.0000101	---
U238	0.0074055	0.0146475	0.0145302	0.0074012	0.0146470	0.0145302
P	0.0000158	0.0000056	0.0000100	0.0000158	0.0000056	0.0000100
S	0.0000138	0.0000012	0.0000079	0.0000138	0.0000012	0.0000079
Cl	0.0000003	0.0000003	0.0000003	0.0000003	0.0000003	0.0000003
Ca	0.0000019	0.0000021	0.0000021	0.0000019	0.0000021	0.0000021
Co	0.0000017	0.0000011	0.0000008	0.0000017	0.0000011	0.0000008
LIP	0.0000028	0.0000016	0.0000016	0.0000028	0.0000016	0.0000016
HIP	0.0000018	0.0000011	0.0000011	0.0000018	0.0000011	0.0000011

TABLE 2.2. **(contd)**

	Master 925			Master 926		
Isotopes[a]	0-18	18-18*	18-31	0-18	18-18*	18-31
C	0.0000677	0.0000350	0.0000638	0.0000677	0.0000350	0.0000638
O	0.0000007	0.0000006	0.0000007	0.0000007	0.0000006	0.0000007
Na	0.0092797	0.0093249	0.0093062	0.0092797	0.0093249	0.0093062
Si	0.0002704	0.0001653	0.0003084	0.0002704	0.0001653	0.0003110
Al	0.0000028	0.0000028	0.0000028	0.0000028	0.0000028	0.0000028
Mn	0.0004462	0.0002169	0.0003738	0.0004462	0.0002169	0.0003760
Cr	0.0050861	0.0025463	0.0040831	0.0050861	0.0025463	0.0041057
Fe	0.0181576	0.0090956	0.0142331	0.0181576	0.0090956	0.0143100
Ni	0.0023045	0.0010941	0.0017580	0.0023045	0.0010941	0.0017680
Cu	0.0000297	0.0000283	0.0000278	0.0000297	0.0000283	0.0000278
Zr	0.0000001	---	---	0.0000001	---	---
Mo	0.0000146	0.0000149	0.0000126	0.0000146	0.0000149	0.0000126
U234	0.0000218	0.0000216	---	0.0000218	0.0000216	---
U235	0.0022350	0.0022291	0.0000324	0.0022348	0.0022291	0.0000324
U236	0.0000104	0.0000103	---	0.0000104	0.0000103	---
U238	0.0073783	0.0146799	0.0145458	0.0073994	0.0146799	0.0145458
P	0.0000125	0.0000058	0.0000116	0.0000125	0.0000058	0.0000116
S	0.0000038	0.0000013	0.0000056	0.0000038	0.0000013	0.0000056
Cl	0.0000003	0.0000003	0.0000003	0.0000003	0.0000003	0.0000003
Ca	0.0000021	0.0000021	0.0000021	0.0000021	0.0000021	0.0000021
Co	0.0000013	0.0000013	0.0000008	0.0000013	0.0000013	0.0000008
LIP	0.0000016	0.0000016	0.0000016	0.0000016	0.0000016	0.0000016
HIP	0.0000011	0.0000011	0.0000011	0.0000011	0.0000011	0.0000011

TABLE 2.2. **(contd)**

	Master 927			Master 928		
Isotopes[a]	0-18	18-18*	18-31	0-18	18-18*	18-31
C	0.0000677	0.0000350	0.0000638	0.0000781	0.0000342	0.0000669
O	0.0000007	0.0000006	0.0000007	0.0000006	0.0000006	0.0000007
Na	0.0092797	0.0093249	0.0093062	0.0083220	0.0093249	0.0093062
Si	0.0002704	0.0001653	0.0003084	0.0002691	0.0001497	0.0002721
Al	0.0000028	0.0000028	0.0000028	0.0000049	0.0000028	0.0000028
Mn	0.0004462	0.0002169	0.0003738	0.0005125	0.0002116	0.0004194
Cr	0.0050861	0.0025463	0.0040831	0.0063880	0.0024798	0.0049151
Fe	0.0181576	0.0090956	0.0142331	0.0226262	0.0088597	0.0173091
Ni	0.0023045	0.0010941	0.0017580	0.0027197	0.0010672	0.0020853
Cu	0.0000297	0.0000283	0.0000278	0.0000608	0.0000281	0.0000423
Zr	0.0000001	---	---	0.0000001	---	---
Mo	0.0000146	0.0000149	0.0000126	0.0000567	0.0000141	0.0000330
U234	0.0000218	0.0000216	---	0.0000213	0.0000211	---
U235	0.0022350	0.0022291	0.0000324	0.0021858	0.0021871	0.0000326
U236	0.0000104	0.0000103	---	0.0000102	0.0000101	---
U238	0.0073892	0.0146799	0.0145598	0.0073889	0.0146475	0.0145302
P	0.0000125	0.0000058	0.0000116	0.0000158	0.0000055	0.0000132
S	0.0000038	0.0000013	0.0000056	0.0000138	0.0000011	0.0000101
Cl	0.0000003	0.0000003	0.0000003	0.0000003	0.0000003	0.0000003
Ca	0.0000021	0.0000021	0.0000021	0.0000019	0.0000021	0.0000021
Co	0.0000013	0.0000013	0.0000008	0.0000017	0.0000011	0.0000008
LIP	0.0000016	0.0000016	0.0000016	0.0000028	0.0000016	0.0000016
HIP	0.0000011	0.0000011	0.0000011	0.0000018	0.0000011	0.0000011

TABLE 2.2. (contd)

	Master 929 and 930		
Isotopes[a]	0-18	18-18*	18-31
C	0.0000710	0.0000342	0.0000515
O	0.0000006	0.0000006	0.0000007
Na	0.0083220	0.0093249	0.0093062
Si	0.0002381	0.0001497	0.0001887
Al	0.0000049	0.0000028	0.0000028
Mn	0.0004422	0.0002116	0.0003341
Cr	0.0054447	0.0024798	0.0040597
Fe	0.0193444	0.0088597	0.0144338
Ni	0.0023300	0.0010672	0.0017164
Cu	0.0000530	0.0000281	0.0000423
Zr	0.0021391	---	---
Mo	0.0000411	0.0000141	0.0000330
U234	0.0000213	0.0000211	---
U235	0.0021858	0.0021871	0.0000326
U236	0.0000102	0.0000101	---
U238	0.0074134	0.0146475	0.0145302
P	0.0000126	0.0000055	0.0000100
S	0.0000073	0.0000011	0.0000079
Cl	0.0000003	0.0000003	0.0000003
Ca	0.0000019	0.0000021	0.0000021
Co	0.0000017	0.0000011	0.0000008
LIP	0.0000028	0.0000016	0.0000016
HIP	0.0000018	0.0000011	0.0000011

[a]LIP refers to impurities of atomic mass less than 23 and HIP refers to impurities of atomic mass greater than 23. The axial composition regions are given to the nearest inch for brevity and 18* refers to 18.36 inches.

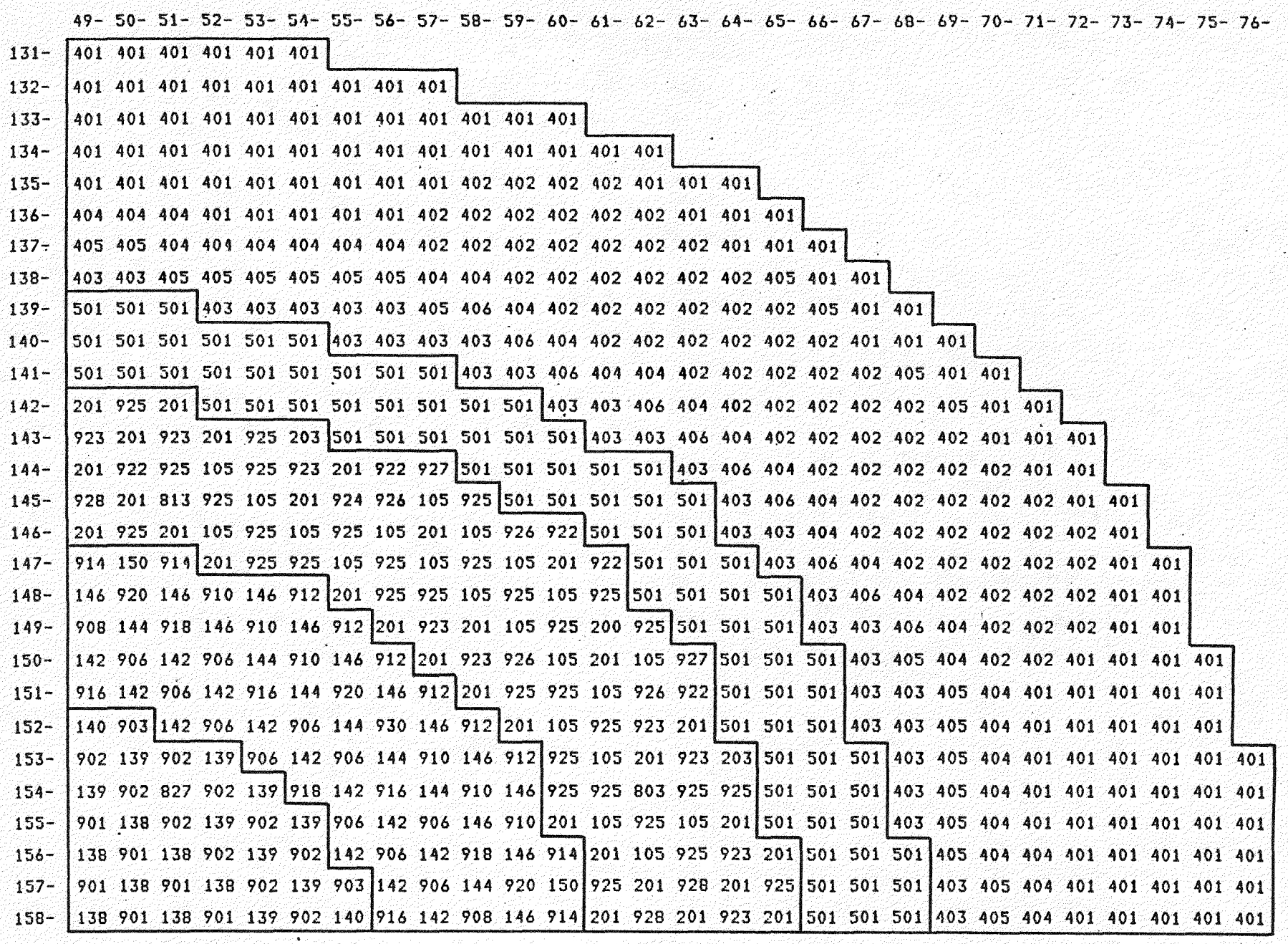

Fig. 2.1. Calculation Model for ZPPR-15C in xy Geometry.

3. MULTIGROUP CROSS SECTION DATA AND CALCULATION MODELS FOR ZPPR-15D

(G. L. Grasseschi and P. J. Collins)

In ZPPR-15D, approximately 90% of the core drawers contained ^{235}U fuel and the remainder contained plutonium fuel. A cross section library in 21 energy groups for uranium fuel was generated using methods consistent with those used for ZPPR-15B (ZPR-TM-470, p. 3 et seq.) and with those used by the IFR design group. The cross section processing may be briefly described as follows:

a. MC^2-II spectrum calculation in 2082 groups, using ENDF/B-V.2 data, for the homogenized composition of the inner core region. The input parameters were -- consistent P1, screened diluent isotopes, 20 resolved resonances in overlap treatment, thermal group cross sections added, buckling search to critical with collapse to 230 intermediate groups.

b. Cell calculations using the 230 group intermediate data in the SDX code were made for the principal uranium-fuelled cells:

- single-fuel-column, 1/16 in. enriched uranium, symmetric Zr, symmetric uranium (SCS)
- single-fuel-column, 1/16 in. enriched uranium, asymmetric Zr, asymmetric uranium (SCA)
- single-fuel-column, 1/8 in. enriched uranium (SDC)
- double-fuel-column, 2 x 1/16 in. enriched uranium (DC)
- single-fuel-column, 1/16 in. enriched uranium, no Zr (SC)
- radial blanket cell (RB)
- homogeneous radial reflector (RR)
- axial blanket cell (AB)
- sodium-voided, single-fuel-column, 1/16 in. enriched uranium, symmetric Zr (SCSV)

c. Collapse of the cross sections to 21 groups was made with cylindrical diffusion models as in ZPPR-15B (ZPR-TM-470). The region boundaries were 379 mm (symmetric Zr zone), 660 mm (inner

core), 933 mm (outer core), 1091 mm (radial blanket) and 1555 mm radial reflector. Four calculations were made with the following regions (cells):

1. |SCS|SCA|DC SDC DC SDC DC|RB|RR|

This model provided most of the cross sections required;

2. |SCS|SCA|DC SC DC SC DC|RB|RR|

This model provided data for single-fuel-column cells in the outer core (SC);

3. |SDSV|SCS|SCA|DC SDC DC SDC DC|RB|AB|

This model provided data for the central sodium-void zone (SCSV) and its surrounding zone (SCS) for sodium void analysis;

4. |SCS|SCA|DC SDC DC SDC DC|AB|AR|

This model provided data for the axial blanket and axial reflector (IFR design method).

Limitations of the SEF collapsing system in the SDX code precluded collapse of each outer core cell over the outer core spectrum and data for the three cell types (DC, SDC and SC) were taken from the central double-fuel-column cell and the single fuel column cell to the left.

A number of the single-fuel-column cells in the inner core (the SCA type) had the uranium fuel placed off-center by 1/32 in. (ZPR-TM-471, p. 3 et seq.). Cell calculations were not made for these types and the isotopic cross sections used were generated for the standard single-fuel-column cells.

The inner core of ZPPR-15D contained several 1/8 in. enriched uranium fuel-column cells (SDC). Cross sections used for these cells were those collapsed in the outer core spectrum.

d. Anisotropic diffusion coefficient modifiers for the DIF3D code were generated by the Benoist method for each of the cell types listed in (a).

As mentioned in Section 2, the plutonium fuel was not included in the ZPPR-15D cross section processing. Data for these cell types were copied from the ZPPR-15B library. This procedure is consistent with that used in IFR design for post-uranium-start-up cores.

The standard calculation model for ZPPR-15D was a 1/8-core xyz description with compositions of all drawer-master variants included except for asymmetric fission chamber and thermocouple drawers. The midplane map of the model is given in Fig. 3.1. The core height was defined by the height of the uranium fuel columns, with mixing in the top 2.33 in. of the core as discussed for ZPPR-15C in Section 2. A list of drawer masters used in 15D is given in Table 3.1. Compositions for drawers not included in 15B and 15C are given in Table 3.2. The axial node spacing in the core region was 4.03 in., 8.03 in., 12.03 in., 16.03 in., and 18.36 inches.

Two calculations were made with an rz-geometry model of ZPPR-15D to estimate the effect of smearing compositions at the top of the core. One model had the axial description used in the xyz calculations and the other explicitly included compositions in the range of 16.03 in. to 18.03 in. and in 18.03 in. to 18.36 inches. Both models had the same finite-difference mesh to minimize truncation errors. The k-effective values differed by only 0.05%, indicating a reasonably small error in the reference xyz model.

TABLE 3.1. Drawer Masters for ZPPR-15D

Zone	Drawer Master	Description
Inner Core (central 148 drawers)	901	Fuel - SC 1/16 U - Symmetric Zr
	902	Fuel - SC 1/16 U - Symmetric Zr
	903	Fuel - SC 1/16 U - Symmetric Zr
	735	Fuel - SC 1/16 U - Symmetric Zr-FC
	863,864	Fuel - SC 1/16 U - Symmetric Zr-PSR
Inner Core	141,142	Fuel - SC Pu - Asymmetric Zr
	143,144	Fuel - SC Pu - Asymmetric Zr
	145,146	Fuel - SC Pu - Asymmetric Zr
	905,906	Fuel - SC 1/16 U - Asymmetric Zr
	907,908	Fuel - SC 1/16 U - Asymmetric Zr
	909,910	Fuel - SC 1/16 U - Asymmetric Zr
	911,912	Fuel - SC 1/16 U - Asymmetric Zr
	913,914	Fuel - SC 1/16 U - Asymmetric Zr
	915,916	Fuel - SC 1/8 U - Asymmetric Zr
	917,918	Fuel - SC 1/8 U - Asymmetric Zr
	919,920	Fuel - SC 1/8 U - Asymmetric Zr
	929,930	Fuel - SC 1/8 U - Asymmetric Zr
	937,938	Fuel - SC 1/8 U - Asymmetric Zr
	714	Fuel - SC Pu - Asymmetric Zr-FC
	736,737	Fuel - SC 1/16 U - Asymmetric Zr-FC
	738	Fuel - SC 1/8 U - Asymmetric Zr-FC
	743	Fuel - SC 1/8 U - Asymmetric Zr-FC
Outer Core	201	Fuel - DC Pu
	921,922	Fuel - SC 1/16 U - Asymmetric
	923	Fuel - SC 1/8 U
	924	Fuel - SC 1/8 U
	925	Fuel - DC 1/16 U
	926	Fuel - DC 1/16 U
	927	Fuel - DC 1/16 U
	928	Fuel - SC 1/8 U
	935	Fuel - SC 1/8 U
	936	Fuel - DC 1/16 U
	703	Fuel - DC Pu-FC
	707	Fuel - DC Pu-Thermocouple
	739,740	Fuel - SC 1/16 U - Asymmetric-FC
	741	Fuel - DC 1/16 U - FC
	742	Fuel - SC 1/8 U - FC
	865,866	Fuel - SC 1/16 U - PSR
Radial Blanket	501	DU
	704	DU-FC

TABLE 3.1. **(contd)**

Zone	Drawer Master	Description
Radial Reflector	401	Stainless Steel
	402	Stainless Steel
	403	Stainless Steel
	404	Stainless Steel
	405	Stainless Steel
	406	Stainless Steel
	704	Stainless Steel - FC

SC - single fuel column
Pu - ZPPR Pu/U/Mo fuel
U - 93% enriched uranium metal fuel
DU - depleted uranium metal
DC - double fuel column
FC - fission chamber
PSR - narrow drawer adjacent to poison rod or shim rod

TABLE 3.2. ZPPR Assembly 15D -- Atom Densities (atoms/barn-cm)

	Master 935			Master 936		
Isotopes[a]	0-18	18-18*	18-31	0-18	18-18*	18-31
B-10	---	---	---	---	---	---
B-11	---	---	---	---	---	---
C	0.0000781	0.0000342	0.0000515	0.0000677	0.0000350	0.0000638
O	0.0000006	0.0000006	0.0000007	0.0000007	0.0000006	0.0000007
Na	0.0083220	0.0093249	0.0093062	0.0092797	0.0093249	0.0093062
Si	0.0006911	0.0001497	0.0001887	0.0002704	0.0001653	0.0003110
Al	0.0000049	0.0000028	0.0000028	0.0000028	0.0000028	0.0000028
Mn	0.0005125	0.0002116	0.0003341	0.0004462	0.0002169	0.0003760
Cr	0.0063884	0.0024798	0.0040597	0.0050861	0.0025463	0.0041057
Fe	0.0226274	0.0088597	0.0144338	0.0181576	0.0090956	0.0143100
Ni	0.0027199	0.0010672	0.0017164	0.0023045	0.0010941	0.0017680
Cu	0.0000608	0.0000281	0.0000423	0.0000297	0.0000283	0.0000278
Zr	0.0000001	---	---	0.0000001	---	---
Mo	0.0000567	0.0000141	0.0000330	0.0000146	0.0000149	0.0000126
U234	0.0000217	0.0000211	---	0.0000218	0.0000216	---
U235	0.0022380	0.0021871	0.0000326	0.0022348	0.0022291	0.0000324
U236	0.0000103	0.0000101	---	0.0000104	0.0000103	---
U238	0.0073965	0.0146475	0.0145302	0.0074103	0.0146799	0.0145598
P	0.0000158	0.0000055	0.0000100	0.0000125	0.0000058	0.0000116
S	0.0000138	0.0000011	0.0000079	0.0000038	0.0000013	0.0000056
Cl	0.0000003	0.0000003	0.0000003	0.0000003	0.0000003	0.0000003
Ca	0.0000019	0.0000021	0.0000021	0.0000021	0.0000021	0.0000021
Co	0.0000017	0.0000011	0.0000008	0.0000013	0.0000013	0.0000008
LIP	0.0000028	0.0000016	0.0000016	0.0000016	0.0000016	0.0000016
HIP	0.0000018	0.0000011	0.0000011	0.0000011	0.0000011	0.0000011

TABLE 3.2. (contd)

	Master 937			Master 938		
Isotopes[a]	0-18	18-18*	18-31	0-18	18-18*	18-31
B-10	---	---	---	---	---	---
B-11	---	---	---	---	---	---
C	0.0000817	0.0000342	0.0000515	0.0000817	0.0000342	0.0000515
O	0.0000006	0.0000006	0.0000007	0.0000006	0.0000006	0.0000007
Na	0.0083220	0.0093249	0.0093062	0.0083220	0.0093249	0.0093062
Si	0.0002271	0.0001497	0.0001887	0.0002271	0.0001497	0.0001887
Al	0.0000049	0.0000028	0.0000028	0.0000049	0.0000028	0.0000028
Mn	0.0004466	0.0002116	0.0003341	0.0004466	0.0002116	0.0003341
Cr	0.0054382	0.0024798	0.0040597	0.0054382	0.0024798	0.0040597
Fe	0.0194139	0.0088597	0.0144338	0.0194139	0.0088597	0.0144338
Ni	0.0023258	0.0010672	0.0017164	0.0023258	0.0010672	0.0017164
Cu	0.0000534	0.0000281	0.0000423	0.0000534	0.0000281	0.0000423
Zr	0.0022117	---	---	0.0022117	---	---
Mo	0.0000326	0.0000141	0.0000330	0.0000326	0.0000141	0.0000330
U234	0.0000213	0.0000211	---	0.0000213	0.0000211	---
U235	0.0021857	0.0021871	0.0000326	0.0021857	0.0021871	0.0000326
U236	0.0000102	0.0000101	---	0.0000102	0.0000101	---
U238	0.0074022	0.0146475	0.0145302	0.0074022	0.0146475	0.0145302
P	0.0000118	0.0000055	0.0000100	0.0000118	0.0000055	0.0000100
S	0.0000015	0.0000011	0.0000079	0.0000015	0.0000011	0.0000079
Cl	0.0000003	0.0000003	0.0000003	0.0000003	0.0000003	0.0000003
Ca	0.0000019	0.0000021	0.0000021	0.0000019	0.0000021	0.0000021
Co	0.0000017	0.0000011	0.0000008	0.0000017	0.0000011	0.0000008
LIP	0.0000028	0.0000016	0.0000016	0.0000028	0.0000016	0.0000016
HIP	0.0000018	0.0000011	0.0000011	0.0000018	0.0000011	0.0000011

TABLE 3.2. **(contd)**

	Master 863 and 864		Master 865 and 866	
Isotopes[a]	0-18	0-18	0-18	0-18
B-10	---	0.0095075	---	0.0095075
B-11	---	0.0009616	---	0.0009616
C	0.0000877	0.0027400	0.0000790	0.0027393
O	0.0000004	0.0000004	0.0000004	0.0000004
Na	0.0041599	0.0041599	0.0041599	0.0041599
Si	0.0004250	0.0004250	0.0002603	0.0002603
Al	0.0000025	0.0000025	0.0000025	0.0000025
Mn	0.0005079	0.0005079	0.0005141	0.0005141
Cr	0.0055889	0.0055889	0.0064418	0.0064418
Fe	0.0193768	0.0193768	0.0228318	0.0228318
Ni	0.0024099	0.0024099	0.0027110	0.0027110
Cu	0.0000301	0.0000301	0.0000606	0.0000606
Zr	---	---	---	---
Mo	0.0001548	0.0001548	0.0005828	0.0005828
U234	0.0000109	0.0000109	0.0000109	0.0000109
U235	0.0011293	0.0011293	0.0011293	0.0011293
U236	0.0000052	0.0000052	0.0000052	0.0000052
U238	0.0073371	0.0073371	0.0073371	0.0073371
P	0.0000169	0.0000169	0.0000169	0.0000169
S	0.0000088	0.0000088	0.0000161	0.0000161
Cl	0.0000002	0.0000002	0.0000002	0.0000002
Ca	0.0000010	0.0000010	0.0000010	0.0000010
Co	0.0000010	0.0000010	0.0000010	0.0000010
LIP	0.0000014	0.0000014	0.0000014	0.0000014
HIP	0.0000010	0.0000010	0.0000010	0.0000010

[a]LIP refers to impurities of atomic mass less then 23 and HIP refers to impurities of atomic mass greater than 23. The axial composition regions are given to the nearest inch for brevity and 18* refers to 18.36 inches.

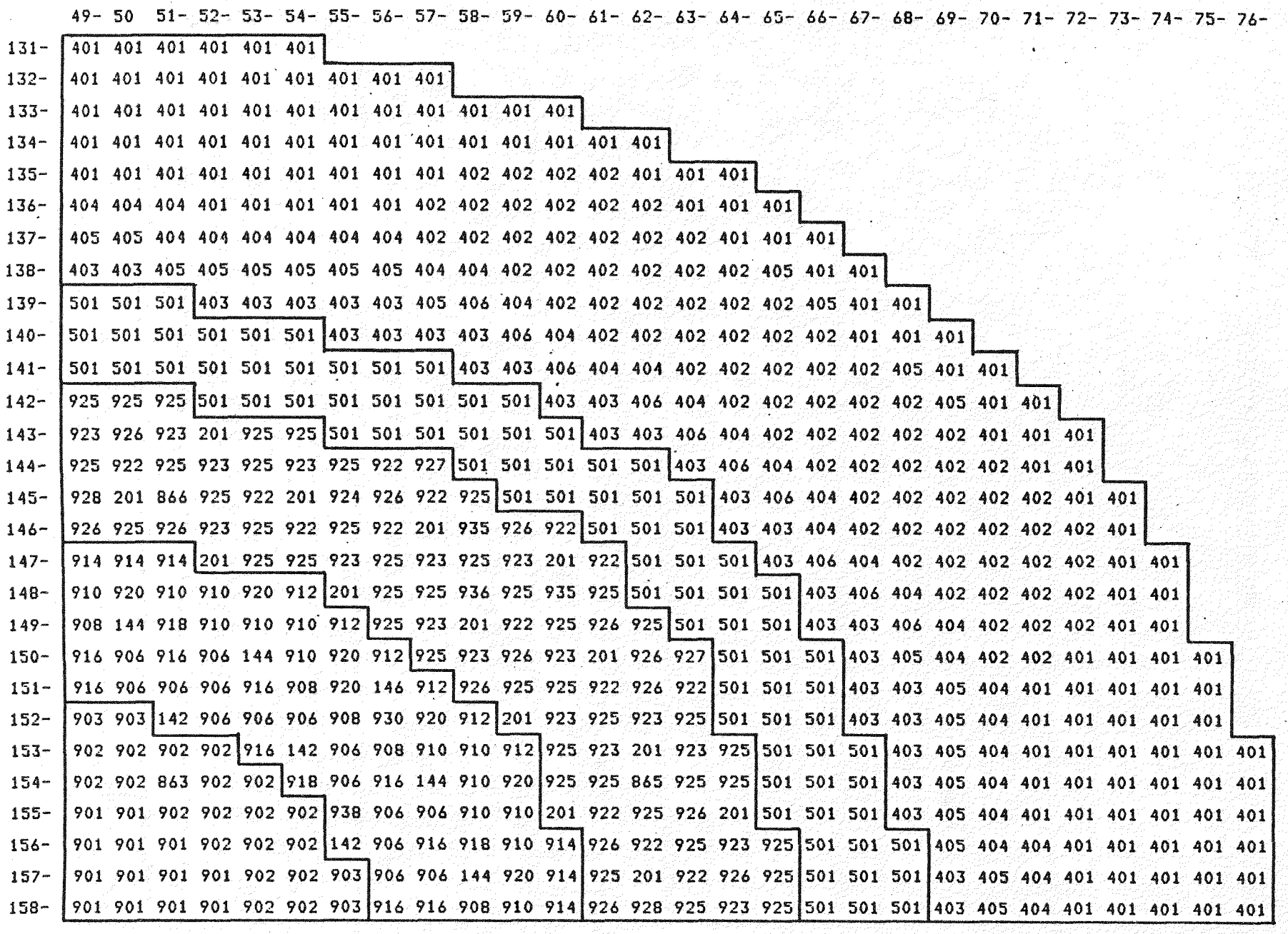

Fig. 3.1. Calculation Model for ZPPR-15D in xy Geometry.

4. CALCULATED K-EFFECTIVE AND DELAYED NEUTRON PARAMETERS FOR ZPPR-15C AND ZPPR-15D (G. L. Grasseschi and P. J. Collins)

The standard calculation method for ZPPR-15 was nodal diffusion theory (NDT) in xyz geometry and 21 group cross sections. Additional calculations were made in xyz finite-difference diffusion theory (FDDT) to calculated delayed neutron parameters with the VARI3D code. For ZPPR-15D, a nodal transport (NTT) calculation was made for comparison with the plutonium-fuelled core ZPPR-15B and for analysis of reaction rates. RZ geometry models were used for both 15C and 15D for economy in some studies. These rz models used zone-average compositions. Since the precise positioning of the fuel cannot be maintained in this homogenization, the eigenvalues are not as accurate as in xyz geometry.

The excess reactivities for ZPPR-15C and ZPPR-15D are given in ZPR-TM-471, p. 4 et seq. The experimental value for k-effective for the 15C critical reference, with shim rods withdrawn and adjusted to a temperature of 293 K, was 1.00052 ± 0.00001. The experimental k-effective for the 15D critical reference was 1.00067 ± 0.00001 and for the 15D subcritical reference was 0.99954 ± 0.00001.

Calculated k-effective values and ratios to experiment are given in Tables 4.1 and 4.2. The FDDT k-effectives are 0.18% (15C) and 0.15% (15D) higher then with NDT due to the coarse (55 mm) mesh employed. For 15D, the C/E results for critical and subcritical references are in good agreement. The nodal transport calculation for 15D increases the k-effective by 0.24% over the NDT value.

Predicted k-effectives for ZPPR-15A, 15B, 15C and 15D are compared in Table 4.3. The transport correction calculated for 15A was applied to 15B based on the similarity of the loadings. A correction of 0.27% Δk, the average of corrections for 15A and 15D, was assumed for 15C. The k-effective for 15D with 90% uranium fuel by volume, is only two tenths of a percent lower than for 15B.

Recent calculations for a matching pair of plutonium oxide fuelled and uranium oxide LMR cores, ZPR-6/7 and ZPR-6/6A,[1] with ENDF/B-V.2 data, and calculation methods similar to those used for ZPPR-15, show a somewhat lower k-effective by 0.4% in the uranium core.

Delayed neutron parameters for ZPPR-15C and 15D were calculated with the FDDT xyz model and the VARI3D editor. Kinetics parameters for the six delayed neutron families are given in Tables 4.4 and 4.5. Effective delayed neutron fractions of 0.5207% in 15C and 0.6564% in 15D compare to 0.3361% in 15B (ZPR-TM-470, p. 21).

REFERENCE

1. C. A. Atkinson and P. J. Collins, "The Performance of ENDF/B-V.2 Data for Fast Reactor Calculations," paper to Topical Meeting on Advances in Reactor Physics, Mathematics and Computation, Paris, April 1987.

TABLE 4.1 Eigenvalue Calculations for ZPPR-15C

Model[a]	Calculated k-effective	Experiment	C/E
NDT xyz	0.992222	1.00052	0.99171
FDDT xyz	0.993984	1.00052	0.99347
FDDT rz	0.992241	1.00052	0.99173

[a]NDT = nodal diffusion, FDDT = finite difference diffusion.

TABLE 4.2 Eigenvalue Calculations for ZPPR-15D

Model[a]	Calculated k-effective	Experiment	C/E
NDT xyz	0.991219	1.00067	0.99056
NTT xyz	0.993622	1.00067	0.99296
FDDT xyz	0.992746	1.00067	0.99208
FDDT rz	0.991521	1.00067	0.99080
NDT xyz[b]	0.990147	0.99954	0.99060

[a]NDT = nodal diffusion, NTT = nodal transport, FDDT = finite difference.

[b]Subcritical reference.

TABLE 4.3. Comparison of Predicted k-effectives (C/Es) for ZPPR-15

Assembly	Diffusion	Transport
ZPPR-15A	0.9927	0.9957
ZPPR-15B	0.9918	0.9948[a]
ZPPR-15C	0.9917	0.9944[b]
ZPPR-15D	0.9906	0.9930

[a]Using transport correction from 15A.

[b]Using transport correction +0.0027 Δk, the mean of 15A and 15D values.

TABLE 4.4 Delayed Neutron Parameters for ZPPR-15C

Family	a_i	λ_i, s^{-1}	$\beta_i, \%$
1	0.02901	0.01283	0.01510
2	0.19966	0.03168	0.10396
3	0.18285	0.12494	0.09521
4	0.38907	0.32811	0.20259
5	0.15619	1.3910	0.08133
6	0.04321	3.8671	0.02250

β-effective 0.5207%.
Prompt neutron lifetime 3.216×10^{-7}.

TABLE 4.5 Delayed Neutron Parameters for ZPPR-15D

Family	a_i	λ_i, s^{-1}	$\beta_i, \%$
1	0.03115	0.01278	0.02044
2	0.19568	0.03178	0.12844
3	0.18161	0.12119	0.11921
4	0.40001	0.32241	0.26257
5	0.15258	1.4012	0.10015
6	0.03898	3.9293	0.02558

β-effective 0.6564%
Prompt neutron lifetime 3.181×10^{-7} s.

5. MEASUREMENTS AND ANALYSIS OF REACTION RATES IN ZPPR-15D

(P. J. Collins, J. M. Gasidlo, G. L. Grasseschi and D. W. Maddison)

5.1 Introduction

ZPPR-15D was a benchmark LMR core with 90% uranium-metal fuel and 10% plutonium-metal fuel. The zone outlines were kept the same as in the three previous cores of ZPPR-15 but the fuel loading increased due to the lower worth of ^{235}U fuel relative to ^{239}Pu fuel. As in ZPPR-15B and 15C, zirconium was present throughout the inner core region but not in the outer core. Reaction rate measurements in ZPPR-15D were made along the x and y axes and along three axial traverses to enable a close comparison to be made with analyses in the earlier cores.

The reference calculations were made with nodal diffusion theory with ENDF/B-V.2 data collapsed to 21 groups and parallel the methods used by the IFR core design group.

5.2 Details of the Measurements

Measurements used the standard techniques with small foils placed between plates of the unit cells. The methods are described in ZPR-TM-469, Section 4. The basic foil data are recorded in Section 6 of this report. As usual, the basic data were adjusted to provide cell-average reaction rates using additional "fine-structure" measurements with multiple foils irradiated in a selected number of unit cells. The uranium cells were basically different from the usual plutonium fuelled cells in that only a small fraction of the ^{238}U was contained in the fuel plates of 93% enriched uranium. Thus, the cell-averaging factors do not require additional input from the mockup fuel plates of the Stanford Robinson experiment. On the other hand, foil/cell-average factors differing by as much as 20% from unity are found for ^{238}U fission in some cells. Details of the fine-structure measurements and derivation of the cell factors are given in Section 7.

The reaction rate measurements were made on June 17, 1986, in loading 203, reactor run 336. Eight ZPPR shim control rods, in location 154-62 and its seven symmetric counterparts were inserted to a depth of 375 mm (14.77 inches) from the midplane, on average, during the irradiation. The rods had a worth of 9.6¢ (0.065 Δk) with respect to the fully-withdrawn position at 755 mm (29.73 inches) from the midplane.

5.3 Calculation Methods

Reaction rates were calculated with an xyz model in nodal diffusion theory using 21 group cross sections and anisotropic diffusion coefficients. Compositions for each drawer master were used in a quarter-xy, half-z model, but asymmetric fission chamber and thermocouple drawers were treated as regular drawers. The model had one node per drawer (55 m x 55 mm) in the xy plane, axial nodes of 102, 102,102,102 and 55 mm in the core and node spacings of about 150 mm in the axial blankets. Cross sections for the uranium-fuelled drawers were processed through MC^2 and SDX and collapsed to 21 groups by the same method as used for the ZPPR-15B library (ZPR-TM-470, p. 13). The cross section processing and reactor model are described in detail in Section 3 of this report.

The ZPPR shim rod blades were not included in the model. Corrections to the reaction rates were taken from ZPPR-15A calculations and scaled by the relative shim rod reactivities in 15D and 15A. The inserted shim rods increased reaction rates by 0.2% at the core center and by 0.3% along the y-axis and depressed reaction rates by 0.2% in the outer core at the x-axis. Axial reaction rates at the top of the core were reduced by 0.6% in position 159-60 and by 1% in position 159-64 (nearest to the shim rods) with reductions of up to 1.5% and 2.5% in the axial blanket at these locations.

The ^{239}Pu fission rates are calculated with infinite-dilution cross sections, generated by adding trace amounts of ^{239}Pu to the uranium cells. Comparisons with foil-shielded cross sections, generated for ZPPR-15A indicates reductions of a few tenths of a percent in calculated fission rates in the core region. These reductions have not been applied.

5.4 Experimental Results and Analysis

Reaction rate distributions for fission in ^{239}Pu and in ^{235}U and for fission and capture in ^{238}U were measured along the x- and y-axes and in three axial traverses; core center, inner core edge and in the outer core. Fission in ^{235}U was also measured on both sides of the core symmetry axes. The measured values and comparisons with calculation are given in Tables 5.1 to 5.7.

The experimental values in the tables are given in units of 10^{-17} fissions or captures per atom per second at a reactor power of approximately 1 watt, as monitored with the ex-core counters. The calculations are normalized so as to give a mean C/E of unity for the 66 measurements of ^{235}U fission in the core regions.

The reaction rate data are grouped according to reactor region, inner core (IC), outer core (OC), radial blanket (RB), and axial blanket (AB). Double-fuel-column drawers are denoted by D and the single-fuel-column drawers with 1/8 in. thick enriched uranium by SD. The remaining locations are single-fuel-column drawers with 1/16 in. thick enriched uranium pieces. The calculated reaction rates are interpolated to the center of the foil using the nodal polynomial coefficients. The positions of the foils within the drawers are given in Section 6 together with the basic (i.e not cell-averaged) data.

A summary of the radial reaction rate analysis is given in Table 5.8. With nodal diffusion calculations, the ^{235}U fission rates are slightly underpredicted in the outer core, by 0.5% on average, relative to the inner core. This trend is more marked for ^{239}Pu fission and ^{238}U capture rates where the mean C/E in the outer core is about 1.5% lower than for the inner core. Standard deviations of the region-averaged C/Es are about 1% for the non-threshold reactions compared with about 0.7% for statistical uncertainties on foil counting (Section 6).

In more detail, several imperfections in the analysis were noted. (1) C/E values in the outer core are persistently lower at the

y-axis than at the x-axis by 1% for ^{235}U fission and ^{238}U capture and by 2% for ^{238}U fission. The most obvious geometric features which differ in these two directions are plate orientation (streaming effects) and shim rod locations. (2) Reaction rates in the two adjacent drawers in the inner core with increased fuel (SD drawers) have notably lower C/E values than their neighbors. For ^{235}U fission, the difference in predictions is 2-3% and is unusual, to say the least, for this reaction in comparison with previous ZPPR analyses. (3) ^{235}U fission rates show a marked increase in C/E of 8% in progressing through the radial blanket. This trend was also seen in ZPPR-15B (ZPR-TM-470, p. 28 et seq.) and appears to be mainly due to treatment of cross sections in the steel reflector.

The results of axial reaction rate analysis are very similar to those found in many previous cores: The non-threshold reaction rates are predicted about 1% low near the top of the core relative to the axial average. However, the C/E values are remarkably constant with penetration of up to 280 mm into the axial blanket. The threshold reaction, ^{238}U fission, exhibits a 20% jump in C/E across the core/axial blanket boundary. This result is entirely expected with fine-mesh diffusion calculations. Results for ^{238}U fission deep in the blanket should not be taken seriously because of the poor experimental statistics.

5.5 Reaction Rate Ratios

The foil data have been combined to give reaction rate ratio data for each of the traverses in Tables 5.9 to 5.13. The notation F5/F9 to represent $^{235}U(n,f)/^{239}Pu(n,f)$ etc., is often used for brevity in the tables. The ratios in the tables are formed simply from the values measured at slightly different xyz locations. However, the calculations are interpolated to the actual foil positions so that the C/E values are appropriate.

Mean C/E values for the reaction rate ratios are given in Table 5.14. The standard deviations of the C/E distributions, for 32 results in the inner core and 11 results in the outer core are consistent with the experimental statistical uncertainties for each foil. The mean

C/E values are significantly higher in the outer core than in the inner core, by 2%, for F5/F9 and F8/F9.

5.6 Transport Calculations

Reaction rates in ZPPR-15D were calculated using the same xyz model with the nodal transport approximation and anisotropic transport cross sections consistent with the diffusion coefficients used in the nodal diffusion calculations. The k-effective for the transport model was 0.24% higher than that for the nodal diffusion model (Section 4).

The reaction rate analysis with transport calculations (C/E results) is shown for the x-axis traverse in Table 5.15 and for the axial traverse at the center in Table 5.16. The ratios of transport to diffusion reaction rates are also shown in the tables. Transport effects are similar for the other traverses and are not shown explicitly.

The transport effects in ZPPR-15D are quite small, of the order of 1%, except for fission in ^{238}U. The principal effects are

(i) A flattening of the calculated radial distributions. Plutonium fission rates and uranium capture rates are consistently predicted in the inner core and outer core. The ^{235}U fission rate is a little overpredicted in the outer core.

(ii) The ^{238}U fission rates are much improved across the core/blanket interfaces. Discrepancies of 15% (radial) and 20% (axial) by diffusion theory are reduced to 5% and 8% respectively. Previous analyses of heterogeneous core show that this discrepancy could be further reduced by about 5% by treatment of coupled core/blanket cells in the cell heterogeneity calculations.

(iii) The ^{238}U fission rates are predicted more consistently between single and double fuel-column cells. However the discrepancy in prediction in the outer core relative to the inner core is increased for this reaction.

(iv) ^{235}U fission rates in the anomalous (SD) drawers in the inner core are only marginally improved (0.5%) and remain about 2% discrepant relative to their neighbors.

Reaction rate ratio C/E results are given in Table 5.17. The F5/F9 results are minimally different to those from the diffusion analysis and remain 1.5% higher in the outer core. The C8/F9 results are consistent between the two core zones due to a reduction of 0.5% in the outer core but the discrepancy in F8/F9 is increased to 3.7%.

5.7 Summary

Reaction rate distributions in ZPPR-15D are generally quite well predicted. With diffusion calculations, the C/E results in the outer core are no more than 2% lower than in the inner core, on average, and are improved by about 1% by transport calculations. In the axial direction, calculated values are underestimated by about 1% at the top of the core, relative to the axial average and show consistent C/E values as far as 280 mm (11 in.) into the axial blanket.

Reaction rates through the thin radial blanket show a marked trend of increasing C/E for ^{235}U fission and decreasing C/E for ^{238}U fission, although calculation of the latter reaction is also effected by treatment of boundary cells. This problem appears to be due principally to treatment of the steel radial reflector as shown by the more extensive data for ZPPR-15A (ZPR-TM-469, p. 5 et seq.).

Reaction rates around the cells with double fuel content (DC and SDC cells) are more discrepant than in previous analyses of ZPPR. This is unusual for ^{235}U fission in particular. The uranium cells are more heterogeneous than the plutonium cells (Section 7). It is possible that treatment of multiple cells in the SDX code would improve he analysis.

A comparison of analyses for the uranium fuelled core, ZPPR-15D, with the plutonium fuelled core, ZPPR-15B, is appropriate (Table 5.18). The apparent improvement in radial distributions in 15D, however, may be

due to inadequacies in cell processing in the outer core rather than to nuclear data. The C/Es for reaction rate ratios in 15D are 1% to 2% higher in 15D than in 15B.

TABLE 5.1. ZPPR-15D: Measurements of $^{235}U(n,f)$ along the x-axis

RHS of Matrix				LHS of Matrix			
Matrix	Region[a]	Exp.	C/E	Matrix	Region[a]	Exp.	C/E
159 49	IC[b]	1.433	1.000	159 48	IC	1.431	1.007
159 50	IC	1.445	0.998	159 47	IC	1.453	0.993
159 51	IC	1.435	1.007	159 46	IC	1.448	0.998
159 52	IC	1.438	1.007	159 45	IC	1.446	1.002
159 53	IC	1.456	1.000	159 44	IC	1.447	1.006
159 54	IC	1.441	1.010	159 43	IC	1.442	1.010
159 55	IC	1.429	1.013	159 42	IC	1.435	1.008
159 56	IC SD	1.424	0.981	159 41	IC SD	1.421	0.983
159 57	IC SD	1.400	0.980	159 40	IC SD	1.397	0.983
159 58	IC	1.354	1.007	159 39	IC	1.354	1.007
159 59	IC	1.292	1.014	159 38	IC	1.293	1.013
159 60	IC[b]	1.217	1.011	159 37	IC	1.221	1.014
Region IC Mean C/E			1.002	Region IC Mean C/E			1.002
S.D.			0.011	S.D.			0.011
159 61	OC D	1.155	1.003	159 36	OC D	1.156	1.002
159 62	OC SD	1.047	1.007	159 35	OC SD	1.054	1.000
159 63	OC D	0.955	1.002	159 34	OC D	0.958	0.998
159 64	OC SD[b]	0.816	0.992	159 33	OC SD	0.811	0.997
159 65	OC D	0.694	1.015	159 32	OC D	0.695	1.014
Region OC Mean C/E			1.004	Region OC Mean C/E			1.002
S.D.			0.008	S.D.			0.007
159 66	RB	0.559	1.016	159 31	RB	0.558	1.019
159 67	RB	0.449	1.038	159 30	RB	0.450	1.035
159 68	RB	0.393	1.097	159 29	RB	---	---
Region RB Mean C/E			1.050	Region RB Mean C/E			1.027

[a]Region IC = Inner Core, OC = Outer Core, RB = Radial Blanket. Fuel drawers with higher uranium content are denoted by SD for one 1/8 in. column and by D for two 1/16 in. columns. The remaining fuel drawers along the axis have one 1/16 in. fuel column. S.D. is the standard deviation of the C/E distribution for the region.

[b]Axial traverse location.

TABLE 5.2. ZPPR-15D: Measurements of $^{239}Pu(n,f)$, $^{238}U(n,\gamma)$ and $^{238}U(n,f)$ along the x-axis

		$^{239}Pu(n,f)$		$^{238}U(n,\gamma)$		$^{238}U(n,f)$	
Matrix	Region[a]	Exp.	C/E	Exp.	C/E	Exp.	C/E
159 49	IC[b]	1.501	0.985	0.1818	1.044	0.02775	0.988
159 50	IC	1.459	1.008	0.1825	1.041	0.02805	0.980
159 51	IC	1.482	0.995	0.1827	1.041	0.02782	0.994
159 52	IC	1.495	0.990	0.1826	1.042	0.02843	0.983
159 53	IC	1.498	0.994	0.1815	1.048	0.02863	0.988
159 54	IC	1.503	0.995	0.1816	1.042	0.02915	1.000
159 55	IC	1.468	1.020	0.1769	1.052	0.03033	1.019
159 56	IC SD	1.517	0.984	0.1763	1.022	0.03602	0.945
159 57	IC SD	1.501	0.982	0.1711	1.028	0.03555	0.965
159 58	IC	1.419	1.012	0.1692	1.023	0.03417	0.988
159 59	IC	1.390	0.995	0.1617	1.025	0.03261	0.996
159 60	IC[b]	1.337	0.990	0.1505	1.031	0.03226	1.004
Region IC Mean C/E			0.996		1.037		0.988
S.D.			0.012		0.010		0.019
159 61	OC D	1.250	0.993	0.1410	1.030	0.03275	1.000
159 62	OC SD	1.167	0.958	0.1278	1.010	0.03223	0.991
159 63	OC D	1.046	0.989	0.1143	1.036	0.02937	0.999
159 64	OC SD[b]	0.913	0.963	0.0985	1.020	0.02462	0.974
159 65	OC D	0.745	1.009	0.0860	1.036	0.01952	1.000
Region OC Mean C/E			0.982		1.026		0.993
S.D.			0.021		0.011		0.011
159 66	RB	0.574	1.006	0.0691	1.035	0.00899	1.149
159 67	RB	0.440	1.018	0.0561	1.038	0.00417	1.050
159 68	RB	0.384	1.006	0.0464	1.060	0.00225	0.863
Region RB Mean C/E			1.010		1.044		1.021

[a]Region IC = inner core, OC = outer core, RB = radial blanket. Fuel drawers with higher uranium content are denoted by SD for one 1/8 in. column and by D for two 1/16 in. columns. The remaining fuel drawers along the axis have one 1/16 in. fuel column. S.D. is the standard deviation of the C/E distribution for the region.

[b]Axial traverse location.

TABLE 5.3. ZPPR-15D: Measurements of $^{235}U(n,f)$ along the y-axis

Upper Half of Matrix				Lower Half of Matrix			
Matrix	Region[a]	Exp.	C/E	Matrix	Region[a]	Exp.	C/E
158 49	IC	1.433	1.005	159 49	IC	1.433	1.000
157 49	IC	1.449	0.995	160 49	IC	1.442	1.000
156 49	IC	1.439	1.002	161 49	IC	1.443	1.000
155 49	IC	1.445	0.999	162 49	IC	1.389	1.039
154 49	IC	1.425	1.017	163 49	IC	1.444	1.004
153 49	IC	1.437	1.007	164 49	IC	1.435	1.009
152 49	IC	1.428	1.007	165 49	IC	1.426	1.008
151 49	IC SD	1.406	0.987	166 49	IC SD	1.401	0.991
150 49	IC SD	1.390	0.982	167 49	IC SD	1.372	0.994
149 49	IC	1.347	1.007	168 49	IC	1.354	1.002
148 49	IC	1.293	1.009	169 49	IC	1.288	1.013
147 49	IC	1.233	1.001	170 49	IC	1.215	1.016
Region IC Mean C/E			1.002	Region IC Mean C/E			1.006
S.D.			0.010	S.D.			0.013
146 49	OC D	1.148	0.986	171 49	OC D	1.143	0.990
145 49	OC SD	1.047	1.008	172 49	OC SD	1.045	1.010
144 49	OC D	0.935	0.988	173 49	OC D	0.930	0.993
143 49	OC SD	0.816	0.997	174 49	OC SD	0.813	1.001
142 49	OC D	0.689	0.976	175 49	OC D	0.685	0.982
Region OC Mean C/E			0.991	Region OC Mean C/E			0.995
S.D.			0.012	S.D.			0.011
141 49	RB	0.554	1.016	176 49	RB	0.553	1.018
140 49	RB	0.452	1.032	177 49	RB	0.452	1.032
139 49	RB	0.400	1.105	178 49	RB	0.401	1.105
Region RB Mean C/E			1.051	Region RB Mean C/E			1.052

[a]Region IC = inner core, OC = outer core, RB = radial blanket. Fuel drawers with higher uranium content are denoted by SD for one 1/8 in. column and by D for two 1/16 in. columns. The remaining fuel drawers along the axis have one 1/16 in. fuel columns. S.D. is the standard deviation of the C/E distribution for the region.

TABLE 5.4. ZPPR-15D: Measurements of $^{239}Pu(n,f)$, $^{238}U(n,\gamma)$ and $^{238}U(n,f)$ along the y-axis

		$^{239}Pu(n,f)$		$^{238}U(n,\gamma)$		$^{238}U(n,f)$	
Matrix	Region[a]	Exp.	C/E	Exp.	C/E	Exp.	C/E
158 49	IC	1.480	0.992	0.1834	1.036	0.02803	0.978
157 49	IC	1.455	1.009	0.1818	1.044	0.02811	0.977
156 49	IC	1.500	0.981	0.1819	1.043	0.02808	0.983
155 49	IC	1.475	1.000	0.1812	1.045	0.02852	0.975
154 49	IC	1.482	0.999	0.1805	1.049	0.02825	0.995
153 49	IC	1.489	0.997	0.1791	1.050	0.02859	1.009
152 49	IC	1.482	1.003	0.1755	1.053	0.03018	1.012
151 49	IC SD	---	---	0.1744	1.028	0.03559	0.947
150 49	IC SD	---	---	0.1695	1.032	0.03543	0.959
149 49	IC	---	---	0.1668	1.033	0.03308	1.015
148 49	IC	---	---	0.1600	1.032	0.03226	1.005
147 49	IC	---	---	0.1504	1.028	0.03185	1.018
Region IC Mean C/E			0.997		1.039		0.989
S.D.			0.009		0.009		0.023
146 49	OC D	---	---	0.1384	1.018	0.03416	0.963
145 49	OC SD	---	---	0.1272	1.015	0.03182	0.994
144 49	OC D	---	---	0.1137	1.005	0.02916	0.968
143 49	OC SD	---	---	0.0991	1.014	0.02418	0.976
142 49	OC D	---	---	0.0848	1.012	0.01810	0.962
Region OC Mean C/E			---		1.013		0.973
S.D.			---		0.005		0.013
141 49	RB	---	---	0.0693	1.023	0.00852	1.092
140 49	RB	---	---	0.0562	1.031	0.00395	1.036
139 49	RB	---	---	0.0469	1.060	0.00207	0.884
Region RB Mean C/E			---		1.038		1.004

[a]Region IC = inner core, OC = outer core, RB = radial blanket. Fuel drawers with higher uranium content are denoted by SD for one 1/8 in. column and by D for two 1/16 in. columns. The remaining fuel drawers along the axis have one 1/16 in. fuel columns. S.D. is the standard deviation of the C/E distribution for the region.

TABLE 5.5. ZPPR-15D: Axial Traverses in Matrix 159-49 (Core Center)

		^{239}Pu(n,f)		^{235}U(n,f)		^{238}U(n,γ)		^{238}U(n,f)	
Region[a]	z(mm)	Exp.	C/E	Exp.	C/E	Exp.	C/E	Exp.[b]	C/E
IC	77.0	1.501	0.985	1.433	1.000	0.1818	1.044	0.02775	0.988
IC	127.8	1.451	0.988	1.388	1.002	0.1775	1.038	0.02692	0.988
IC	178.6	1.371	0.999	1.339	0.992	0.1689	1.044	0.02594	0.977
IC	254.8	1.246	0.991	1.197	1.003	0.1534	1.042	0.02318	0.981
IC	331.0	1.090	0.976	1.056	0.984	0.1346	1.034	0.02001	0.958
IC	381.8	0.954	0.978	0.928	0.988	0.1214	1.022	0.01756	0.918
IC	432.6	0.826	0.965	0.809	0.975	0.1049	1.033	0.01291	0.952
Region IC Mean C/E			0.983		0.992		1.037		0.966
S.D.			0.011		0.010		0.008		0.025
AB	483.4	---	---	0.699	0.985	0.0879	1.042	0.00684	1.161
AB	534.2	---	---	0.582	0.988	0.0734	1.052	0.00363	1.180
AB	635.8	---	---	0.387	0.996	0.0503	1.032	0.00129	1.019
AB	737.4	---	---	0.283	1.002	0.0336	1.044	0.00066	0.678
Region AB Mean C/E			---		0.993		1.043		1.010
S.D.			---		0.008		0.008		0.232

[a]Region IC = inner core, OC = outer core, AB = axial blanket. Fuel drawers with higher uranium content are denoted by SD for one 1/8 in. column and by D for two 1/16 in. columns. The remaining fuel drawers along the axis have one 1/16 in. fuel columns. S.D. is the standard deviation of the C/E distribution for the region.

[b]Statistical uncertainties for ^{238}U(n,f) range from 2% to 18% with penetration into the axial blanket.

TABLE 5.6. ZPPR-15D: Axial Traverses in Matrix 159-60 (Inner Core Edge)

		^{239}Pu(n,f)		^{235}U(n,f)		^{238}U(n,γ)		^{238}U(n,f)	
Region[a]	z(mm)	Exp.	C/E	Exp.	C/E	Exp.	C/E	Exp.[b]	C/E
IC	77.0	1.337	0.990	1.217	1.011	0.1505	1.031	0.03226	1.004
IC	127.8	1.277	1.005	1.174	1.017	0.1458	1.032	0.03130	1.004
IC	178.6	1.234	0.990	1.122	1.014	0.1391	1.032	0.02950	1.012
IC	254.8	1.113	0.987	1.021	1.004	0.1261	1.030	0.02712	0.985
IC	331.0	0.952	0.988	0.881	1.002	0.1103	1.024	0.02257	0.993
IC	381.8	0.841	0.973	0.784	0.988	0.0989	1.015	0.01887	0.991
IC	432.6	0.700	0.987	0.665	0.998	0.0839	1.045	0.01462	0.974
Region IC Mean C/E			0.989		1.005		1.030		0.995
S.D.			0.009		0.010		0.009		0.013
AB	483.4	---	---	0.573	0.993	0.0703	1.057	0.00741	1.178
AB	534.2	---	---	0.477	0.991	0.0585	1.073	0.00384	1.199
AB	635.8	---	---	0.314	0.989	0.0399	1.047	0.00121	1.060
AB	737.4	---	---	0.221	1.009	0.0263	1.056	0.00081	0.519
Region AB Mean C/E			---		0.996		1.058		0.989
S.D.			---		0.009		0.011		0.319

[a]Region IC = inner core, OC = outer core, AB = axial blanket. Fuel drawers with higher uranium content are denoted by SD for one 1/8 in. column and by D for two 1/16 in. columns. The remaining fuel drawers along the axis have one 1/16 in. fuel columns. S.D. is the standard deviation of the C/E distribution for the region.

[b]Statistical uncertainties for ^{238}U(n,f) range from 2% to 15% with penetration into the axial blanket.

TABLE 5.7. ZPPR-15D: Axial Traverses in Matrix 159-64 (Outer Core)

		^{239}Pu(n,f)		^{235}U(n,f)		^{238}U(n,γ)		^{238}U(n,f)	
Region[a]	z(mm)	Exp.	C/E	Exp.	C/E	Exp.	C/E	Exp.[b]	C/E
OC SD	77.0	0.913	0.963	0.816	0.992	0.0985	1.020	0.02462	0.974
OC SD	127.8	0.879	0.969	0.782	1.002	0.0958	1.015	0.02395	0.969
OC SD	178.6	0.845	0.961	0.752	0.995	0.0911	1.021	0.02235	0.990
OC SD	254.8	0.745	0.978	0.673	0.999	0.0823	1.019	0.02030	0.974
OC SD	331.0	0.648	0.961	0.581	0.996	0.0714	1.020	0.01707	0.974
OC SD	381.8	0.565	0.960	0.515	0.986	0.0641	1.009	0.01475	0.945
OC SD	432.6	0.477	0.956	0.440	0.984	0.0551	1.029	0.01089	0.963
Region IC Mean C/E			0.964		0.993		1.019		0.970
S.D.			0.007		0.007		0.006		0.014
AB	483.4	---	--	0.372	0.997	0.0452	1.070	0.00527	1.164
AB	534.2	---	--	0.308	1.001	0.0383	1.071	0.00271	1.167
AB	635.8	---	--	0.203	0.997	0.0254	1.076	0.00097	0.873
AB	737.4	---	--	0.147	0.988	0.0176	1.023	0.00082	0.325
Region AB Mean C/E			--		0.996		1.060		0.882
S.D.			--		0.006		0.025		0.396

[a]Region IC = inner core, OC = outer core, AB = axial blanket. Fuel drawers with higher uranium content are denoted by SD for one 1/8 in. column and by D for two 1/16 in. columns. The remaining fuel drawers along the axis have one 1/16 in. fuel columns. S.D. is the standard deviation of the C/E distribution for the region.

[b]Statistical uncertainties for ^{238}U(n,f) range from 3% TO 20% with penetration into the axial blanket.

TABLE 5.8. **ZPPR-15D: Summary of Radial Reaction Rate Analysis**

		Inner Core			Outer Core			Radial Blanket		
Reaction	Traverse	No.	<C/E>	S.D.	No.	<C/E>	S.D.	No.	<C/E>	S.D.
$^{235}U(n,f)$	X LHS	12	1.002	0.011	5	1.002	0.007	2	1.027	---
	X RHS	12	1.002	0.011	5	1.004	0.008	3	1.050	---
	Y UPPER	12	1.002	0.010	5	0.991	0.012	3	1.051	---
	Y LOWER	12	1.006	0.013	5	0.995	0.011	3	1.052	---
	ALL DATA	48	1.003	0.011	20	0.998	0.010	11	1.047	0.037
$^{239}Pu(n,f)$	X RHS	12	0.996	0.012	5	0.982	0.021	3	1.010	---
	Y UPPER	7	0.997	0.009	0	---	---	0	---	---
	ALL DATA	19	0.996	0.011	5	0.982	0.021	3	1.010	---
$^{238}U(n,\gamma)$	X RHS	12	1.037	0.010	5	1.026	0.011	3	1.044	---
	Y UPPER	12	1.039	0.009	5	1.013	0.005	3	1.038	---
	ALL DATA	24	1.038	0.010	10	1.020	0.011	6	1.041	0.015
$^{238}U(n,f)$	X RHS	12	0.988	0.019	5	0.993	0.011	3	1.021	---
	Y UPPER	12	0.989	0.023	5	0.973	0.013	3	1.004	---
	ALL DATA	24	0.988	0.021	10	0.983	0.016	6	1.012	0.113

TABLE 5.9. ZPPR-15D: Reaction Rate Ratios along the x-axis

		F5/F9		C8/F9		F8/F9	
Matrix	Region[a]	Exp.[b]	C/E	Exp.[b]	C/E	Exp.[b]	C/E
159 49	IC	0.955	1.015	0.1211	1.060	0.01849	1.003
159 50	IC	0.990	0.990	0.1251	1.033	0.01923	0.972
159 51	IC	0.968	1.012	0.1233	1.046	0.01877	0.999
159 52	IC	0.962	1.017	0.1221	1.053	0.01902	0.993
159 53	IC	0.972	1.006	0.1212	1.054	0.01911	0.994
159 54	IC	0.959	1.015	0.1208	1.046	0.01939	1.005
159 55	IC	0.973	0.993	0.1205	1.030	0.02066	0.999
159 56	IC SD	0.939	0.997	0.1162	1.039	0.02374	0.960
159 57	IC SD	0.933	0.998	0.1140	1.047	0.02368	0.983
159 58	IC	0.954	0.995	0.1192	1.011	0.02408	0.976
159 59	IC	0.929	1.019	0.1163	1.030	0.02346	1.001
159 60	IC	0.910	1.021	0.1126	1.041	0.02413	1.014
Region IC Mean C/E			1.007		1.041		0.992
S.D.			0.011		0.013		0.016
159 61	OC D	0.924	1.010	0.1128	1.037	0.02620	1.007
159 62	OC SD	0.897	1.051	0.1095	1.054	0.02762	1.034
159 63	OC D	0.913	1.013	0.1093	1.047	0.02808	1.010
159 64	OC SD	0.893	1.030	0.1078	1.059	0.02696	1.011
159 65	OC D	0.932	1.006	0.1155	1.027	0.02632	0.991
Region OC Mean C/E			1.022		1.045		1.011
S.D.			0.019		0.013		0.015
159 66	RB	0.975	1.010	0.1206	1.029	0.01527	1.142
159 67	RB	1.020	1.020	0.1275	1.020	0.00948	1.031
159 68	RB	1.022	1.090	0.1208	1.054	0.00584	0.858
Region RB Mean C/E			1.040		1.034		1.010

[a]Region IC = inner core, OC = outer core, RB = radial blanket. Fuel drawers with higher uranium content are denoted by SD for one 1/8 in. column and by D for two 1/16 in. columns. The remaining fuel drawers along the axis have one 1/16 in. fuel columns. S.D. is the standard deviation of the C/E distribution for the region.

[b]Experimental values are not adjusted to the same foil location in the cell.

TABLE 5.10. ZPPR-15D: Reaction Rate Ratios along the y-axis

		F5/F9		C8/F9		F8/F9	
Matrix	Region[a]	Exp.[b]	C/E	Exp.[b]	C/E	Exp.[b]	C/E
158 49	IC	0.968	1.013	0.1239	1.044	0.01894	0.986
157 49	IC	0.996	0.986	0.1249	1.035	0.01932	0.968
156 49	IC	0.959	1.021	0.1213	1.063	0.01872	1.002
155 49	IC	0.980	0.999	0.1228	1.045	0.01934	0.975
154 49	IC	0.962	1.018	0.1218	1.050	0.01906	0.996
153 49	IC	0.965	1.010	0.1203	1.053	0.01920	1.012
152 49	IC	0.964	1.004	0.1184	1.050	0.02036	1.009
Region IC Mean C/E			1.007		1.049		0.993
S.D.			0.012		0.009		0.017

[a]Region IC = inner core, OC = outer core, RB = radial blanket. Fuel drawers with higher uranium content are denoted by SD for one 1/8 in. column and by D for two 1/16 in. columns. The remaining fuel drawers along the axis have one 1/16 in. fuel columns. S.D. is the standard deviation of the C/E distribution for the region.

[b]Experimental values are not adjusted to the same foil location in the cell.

TABLE 5.11. ZPPR-15D: Reaction Rate Ratios in Matrix 158-49 (Core Center)

	$^{235}U(n,f)/^{239}Pu(n,f)$			$^{238}U(n,\gamma)/^{239}Pu(n,f)$			$^{238}U(n,f)/^{239}Pu(n,f)$		
z(mm)[a]	Calc.	Exp.	C/E	Calc.	Exp.	C/E	Calc.	Exp.	C/E
77.0	0.969	0.955	1.015	0.1284	0.1211	1.060	0.01855	0.01849	1.003
127.8	0.970	0.957	1.014	0.1285	0.1223	1.051	0.01855	0.01855	1.000
178.6	0.970	0.977	0.993	0.1287	0.1232	1.045	0.01850	0.01892	0.978
254.8	0.973	0.961	1.012	0.1295	0.1231	1.052	0.01841	0.01860	0.990
331.0	0.977	0.969	1.008	0.1309	0.1235	1.060	0.01803	0.01836	0.982
381.8	0.982	0.972	1.010	0.1328	0.1271	1.045	0.01738	0.01840	0.939
432.6	0.990	0.980	1.010	0.1360	0.1270	1.071	0.01593	0.01563	0.987
Region IC Mean C/E			1.009			1.055			0.983
S.D.			0.007			0.009			0.021

[a]Ratios are not adjusted to the same xy locations.

TABLE 5.12. ZPPR-15D: Reaction Rate Ratios in Matrix 159-60 (Inner Core Edge)

	$^{235}U(n,f)/^{239}Pu(n,f)$			$^{238}U(n,\gamma)/^{239}Pu(n,f)$			$^{238}U(n,f)/^{239}Pu(n,f)$		
z(mm)[a]	Calc.	Exp.	C/E	Calc.	Exp.	C/E	Calc.	Exp.	C/E
77.0	0.929	0.910	1.021	0.1172	0.1126	1.041	0.02447	0.02413	1.014
127.8	0.930	0.919	1.012	0.1173	0.1142	1.027	0.02446	0.02451	0.998
178.6	0.931	0.909	1.024	0.1174	0.1127	1.042	0.02444	0.02391	1.022
254.8	0.933	0.917	1.017	0.1182	0.1133	1.043	0.02432	0.02437	0.998
331.0	0.938	0.925	1.014	0.1201	0.1159	1.036	0.02383	0.02371	1.005
381.8	0.946	0.932	1.015	0.1226	0.1175	1.043	0.02283	0.02243	1.018
432.6	0.960	0.950	1.011	0.1270	0.1200	1.058	0.02062	0.02089	0.987
Region IC Mean C/E			1.016			1.041			1.006
S.D.			0.009			0.005			0.013

[a]Ratios are not adjusted to the same xy locations.

TABLE 5.13. ZPPR-15D: Reaction Rate Ratios in Matrix 159-64 (Outer Core)

	$^{235}U(n,f)/^{239}Pu(n,f)$			$^{238}U(n,\gamma)/^{239}Pu(n,f)$			$^{238}U(n,f)/^{239}Pu(n,f)$		
z(mm)[a]	Calc.	Exp.	C/E	Calc.	Exp.	C/E	Calc.	Exp.	C/E
77.0	0.920	0.893	1.030	0.1142	0.1078	1.059	0.02726	0.02696	1.011
127.8	0.920	0.890	1.034	0.1141	0.1090	1.047	0.02724	0.02724	1.000
178.6	0.921	0.890	1.035	0.1145	0.1078	1.062	0.02725	0.02646	1.030
254.8	0.922	0.903	1.021	0.1150	0.1104	1.042	0.02713	0.02724	0.996
331.0	0.928	0.896	1.036	0.1169	0.1102	1.061	0.02667	0.02633	1.013
381.8	0.936	0.911	1.027	0.1194	0.1136	1.051	0.02573	0.02612	0.985
432.6	0.949	0.922	1.029	0.1244	0.1156	1.076	0.02299	0.02283	1.007
Region OC Mean C/E			1.030			1.057			1.006
S.D.			0.005			0.011			0.014

[a]Ratios are not adjusted to the same xy locations.

TABLE 5.14. ZPPR-15D: Summary of Reaction Rate Ratio Analysis

	Inner Core			Outer Core		
Ratio	No.	Mean C/E	S.D.	No.	Mean C/E	S.D.
F5/F9	32	1.009	0.010	11	1.027	0.013
C8/F9	32	1.046	0.012	11	1.052	0.013
F8/F9	32	0.993	0.018	11	1.008	0.014

TABLE 5.15. ZPPR-15D: Analysis of Reaction Rates along the x-axis with Nodal Transport Calculations (NTT) and Comparison with Nodal Diffusion (NDT) Results

		^{239}Pu(n,f)		^{235}U(n,f)		^{238}U(n,γ)		^{238}U(n,f)	
Matrix	Region	NTT C/E	Ratio NTT/NDT	NTT C/E	Ratio NTT/NDT	NTT C/E	Ratio NTT/NDT	NTT C/E	Ratio NTT/NDT
159 49	IC	0.979	0.994	0.994	0.994	1.038	0.994	0.981	0.993
159 50	IC	1.002	0.994	0.992	0.994	1.035	0.994	0.972	0.992
159 51	IC	0.989	0.994	1.001	0.994	1.035	0.994	0.987	0.993
159 52	IC	0.984	0.994	1.002	0.995	1.036	0.994	0.975	0.992
159 53	IC	0.988	0.994	0.995	0.995	1.043	0.995	0.980	0.992
159 54	IC	0.990	0.995	1.005	0.995	1.037	0.996	0.990	0.990
159 55	IC	1.016	0.996	1.009	0.996	1.048	0.997	1.006	0.987
159 56	IC SD	0.988	0.996	0.983	1.002	1.021	0.999	0.976	1.033
158 57	IC SD	0.986	0.996	0.983	1.003	1.027	0.999	0.995	1.031
158 58	IC	1.009	0.997	1.005	0.998	1.023	1.000	0.967	0.979
158 59	IC	0.992	0.997	1.012	0.998	1.026	1.001	0.977	0.981
158 60	IC	0.988	0.998	1.011	1.000	1.033	1.002	0.975	1.025
Region IC Mean C/E		0.993		0.999		1.034		0.982	
S.D.		0.011		0.010		0.008		0.011	
158 61	OC D	0.999	1.006	1.008	1.005	1.033	1.003	1.025	1.025
158 62	OC SD	0.966	1.008	1.015	1.008	1.016	1.006	1.004	1.013
158 63	OC D	0.996	1.007	1.009	1.007	1.041	1.005	1.014	1.015
158 64	OC SD	0.971	1.008	1.000	1.008	1.024	1.004	0.994	1.020
158 65	OC D	1.016	1.007	1.020	1.005	1.038	1.002	1.038	1.038
Region OC Mean C/E		0.990		1.010		1.030		1.015	
S.D.		0.021		0.008		0.010		0.017	
158 66	RB	0.990	0.984	1.005	0.989	1.028	0.993	1.023	0.892
158 67	RB	1.000	0.982	1.024	0.987	1.027	0.989	0.962	0.916
158 68	RB	0.993	0.987	1.084	0.988	1.047	0.987	0.863	1.000
Region RB Mean C/E		0.994		1.038		1.034		0.949	

TABLE 5.16. ZPPR-15D: Analysis of Axial Traverses in Matrix 158-49 (Core Center) with Nodal Transport (NTT) and Comparison with Nodal Diffusion (NDT) Calculations

			^{239}Pu(n,f)		^{235}U(n,f)		^{238}U(n,γ)		^{238}U(n,f)	
Matrix	Region	z(mm)	NTT C/E	Ratio NTT/NDT	NTT C/E	Ratio NTT/NDT	NTT C/E	Ratio NTT/NDT	NTT C/E	Ratio NTT/NDT
158 49	IC	77.0	0.979	0.994	0.994	0.994	1.038	0.994	0.981	0.993
158 49	IC	127.8	0.980	0.994	0.996	0.994	1.032	0.994	0.980	0.992
158 49	IC	178.6	0.993	0.994	0.986	0.994	1.038	0.994	0.970	0.993
158 49	IC	254.8	0.986	0.995	0.998	0.995	1.036	0.994	0.975	0.994
158 49	IC	331.0	0.971	0.995	0.979	0.995	1.028	0.994	0.957	0.999
158 49	IC	381.8	0.974	0.996	0.983	0.995	1.015	0.993	0.925	1.008
158 49	IC	432.6	0.958	0.993	0.967	0.992	1.021	0.990	0.973	1.032
Region IC	Mean C/E		0.977		0.986		1.030		0.966	
	S.D.		0.011		0.011		0.009		0.020	
158 49	AB	483.4	---	---	0.968	0.983	1.027	0.986	1.052	0.908
158 49	AB	534.2	---	---	0.968	0.980	1.034	0.983	1.059	0.897
158 49	AB	635.8	---	---	0.972	0.976	1.009	0.978	1.028	1.009
158 49	AB	737.4	---	---	0.990	0.988	1.028	0.985	0.736	1.086
Region AB	Mean C/E		---	---	0.975		1.025		0.969	
	S.D.		---	---	0.011		0.011		0.156	

TABLE 5.17. ZPPR-15D: Analysis of Reaction Rate Ratio Data with Nodal Transport (NTT) and Comparison with Nodal Diffusion (NDT) Calculations

	Inner Core				Outer Core			
Ratio	No.	Mean C/E	S.D.	Ratio NTT/NDT	No.	Mean C/E	S.D.	Ratio NTT/NDT
F5/F9	32	1.010	0.010	1.001	11	1.026	0.013	0.999
C8/F9	32	1.046	0.011	1.000	11	1.047	0.012	0.995
F8/F9	32	0.988	0.015	0.995	11	1.025	0.014	1.017

TABLE 5.18. Comparison of Reaction Rate Analyses in ZPPR-15D and ZPPR-15B

	C/E (S.D.)	
Parameter	ZPPR-15D	ZPPR-15B
Ratio Mean C/E in OC to Mean C/E in IC:		
Fission Rate in U235	0.995 (0.015)	0.978 (0.010)
Fission Rate in PU239	0.986 (0.024)	0.979 (0.017)
Fission Rate in U238	0.995 (0.026)	0.961 (0.042)
Capture Rate in U238	0.983 (0.015)	0.994 (0.011)
Reaction Rate Ratios in the inner core:		
F5/F9	1.009 (0.010)	1.001 (0.007)
C8/F9	1.046 (0.012)	1.025 (0.009)
F8.F9	0.993 (0.018)	0.978 (0.017)

6. BASIC DATA FOR REACTION RATE MEASUREMENTS IN ZPPR-15D

(D. W. Maddison and J. M. Gasidlo)

Reaction rates were measured for ^{239}Pu, ^{235}U and ^{238}U along the x and y axes in one quadrant plus the symmetrical locations in other quadrants with ^{235}U. Three axial distributions were measured; one at the core center, one at the inner-core/outer-core boundary and one in the outer core. These locations were the same as those for the reference map of ZPPR-15A (ZPR-TM-469, p. 45).

The foils were first placed in special foil holders which were then loaded into the drawers between the vertical columns* of materials. For single-fuel-column drawers, the foil was placed adjacent to the fuel on the side closest to the core center. For double-fuel-column drawers, the foil was placed adjacent to the fuel plate closest to the core center on the side of the plate closest to the drawer center.

In-drawer foil locations were first chosen for matrix half 1, matrix columns $\geq$ 49. Then matrix columns $\leq$ 48 in half 1 and the corresponding positions in half 2 were taken as the mirror positions.

The radial distributions near the reactor midplane were measured with all three foils centered at the mid-height of the drawer at axial position of 63.1 mm from the reactor midplane for the ^{235}U foil, 77.0 mm for the ^{238}U foil and 90.8 mm for the ^{239}Pu foil. In axial distributions, the foils were centered on the axial position with the ^{235}U foil 13.8 mm above, the ^{238}U foil at and the ^{239}Pu foil 13.8 mm below the mid-height of the drawer.

The basic data for the radial and axial distributions are given in Tables 6.1 to 6.3. The uncertainties given in the tables are due to

---

*ZPPR drawers are divided into sixteen 3.175 mm (1/8 in.) wide vertical columns designed by letters A through P. The letter A denotes the column at the left as one faces the drawer. The letters KL, for example, indicate the foil is between columns K and L, and is centered 34.925 mm (1.375 in.) from the left side of the drawer.

counting statistics, foil positioning in the counter system and corrections for other isotopes in the foils. Additional uncertainties due to detector calibrations, deriving in-plate reaction rates and cell-averaging factors are not included in these tables. See ANL-85-44 for a discussion of the first two of these systematic uncertainties. The random uncertainties for the cell-averaging factors are given in Section 7.

TABLE 6.1. Basic Reaction Rate Data for ^{239}Pu and ^{238}U in the Reference Map of ZPPR-15D

Matrix	Loc[a]	$^{239}Pu(n,f)$[b]	σ	$^{238}U(n,f)$[b]	σ	$^{238}U(n,\gamma)$[b]	σ
139 49	FG			0.0020	0.0001	0.0457	0.0003
140 49	FG			0.0038	0.0002	0.0552	0.0004
141 49	FG			0.0083	0.0002	0.0685	0.0004
142 49	CC			0.0210	0.0004	0.0894	0.0005
143 49	HI			0.0317	0.0004	0.1043	0.0006
144 49	CC			0.0339	0.0004	0.1199	0.0006
145 49	HI			0.0417	0.0004	0.1338	0.0007
146 49	CC			0.0397	0.0005	0.1460	0.0008
147 49	HI			0.0365	0.0005	0.1543	0.0008
148 49	HI			0.0370	0.0004	0.1642	0.0008
149 49	HI			0.0379	0.0004	0.1711	0.0009
150 49	HI			0.0475	0.0005	0.1819	0.0009
151 49	HI			0.0477	0.0005	0.1871	0.0010
152 49	HI	1.482	0.010	0.0385	0.0004	0.1960	0.0010
153 49	HI	1.489	0.010	0.0364	0.0004	0.2000	0.0010
154 49	HI	1.482	0.010	0.0360	0.0004	0.2016	0.0010
155 49	HI	1.475	0.010	0.0363	0.0004	0.2024	0.0010
156 49	HI	1.500	0.010	0.0358	0.0004	0.2032	0.0011
157 49	HI	1.456	0.012	0.0358	0.0004	0.2031	0.0010
158 49	HI	1.480	0.011	0.0357	0.0004	0.2048	0.0010
159 50	HI	1.459	0.011	0.0358	0.0004	0.2039	0.0010
159 51	HI	1.482	0.010	0.0355	0.0005	0.2040	0.0010
159 52	HI	1.495	0.010	0.0362	0.0004	0.2039	0.0010
159 53	HI	1.498	0.010	0.0365	0.0004	0.2027	0.0010
159 54	HI	1.503	0.011	0.0371	0.0005	0.2028	0.0011
159 55	HI	1.468	0.010	0.0387	0.0005	0.1976	0.0010
159 56	HI	1.517	0.011	0.0483	0.0005	0.1892	0.0009
159 57	HI	1.501	0.010	0.0476	0.0005	0.1836	0.0010
159 58	HI	1.419	0.011	0.0392	0.0005	0.1737	0.0009
159 59	HI	1.390	0.010	0.0374	0.0004	0.1660	0.0008
159 61	CC	1.250	0.009	0.0377	0.0004	0.1487	0.0008
159 62	HI	1.167	0.009	0.0416	0.0005	0.1345	0.0007
159 63	CC	1.046	0.008	0.0338	0.0004	0.1205	0.0007
159 65	CC	0.745	0.008	0.0224	0.0003	0.0907	0.0005
159 66	FG	0.573	0.006	0.0085	0.0002	0.0683	0.0004
159 67	FG	0.440	0.005	0.0040	0.0002	0.0551	0.0004
159 68	FG	0.384	0.005	0.0022	0.0002	0.0451	0.0003

[a]Drawer column which designates the foil location. Axial displacement from the reactor midplane was 77.0 mm for ^{238}U and 90.8 mm for ^{239}Pu foils.

[b]The data are given in units of 10^{-17} reactions/atom-watt-s. The uncertainties are one standard deviation as discussed in detail in the text.

TABLE 6.2. Basic Reaction Rate Data for ^{235}U in the Reference Map of ZPPR-15D

Matrix	Loc[a]	$^{235}U(n,f)$[b]	σ	Matrix	Loc[b]	$^{235}U(n,f)$[b]	σ
159 29	JK	0.394	0.003	157 49	HI	1.449	0.007
159 30	JK	0.450	0.003	158 49	HI	1.433	0.007
159 31	JK	0.558	0.004	160 49	HI	1.442	0.007
159 32	NN	0.695	0.005	161 49	HI	1.443	0.008
159 33	HI	0.812	0.005	162 49	HI	1.389	0.006
159 34	NN	0.958	0.005	163 49	HI	1.444	0.008
159 35	HI	1.056	0.005	164 49	HI	1.435	0.008
159 36	NN	1.156	0.007	165 49	HI	1.426	0.007
159 37	HI	1.221	0.006	166 49	HI	1.402	0.007
159 38	HI	1.293	0.007	167 49	HI	1.374	0.008
159 39	HI	1.354	0.007	168 49	HI	1.354	0.007
159 40	HI	1.398	0.007	169 49	HI	1.288	0.006
159 41	HI	1.423	0.007	170 49	HI	1.214	0.006
159 42	HI	1.435	0.007	171 49	CC	1.143	0.006
159 43	HI	1.442	0.007	172 49	HI	1.047	0.005
159 44	HI	1.447	0.007	173 49	CC	0.930	0.005
159 45	HI	1.446	0.007	174 49	HI	0.815	0.005
159 46	HI	1.448	0.007	175 49	CC	0.685	0.004
159 47	HI	1.453	0.007	176 49	FG	0.553	0.003
159 48	HI	1.431	0.007	177 49	FG	0.452	0.003
131 49	HI	0.081	0.001	178 49	FG	0.401	0.003
132 49	HI	0.148	0.002	159 50	HI	1.445	0.006
133 49	HI	0.222	0.002	159 51	HI	1.435	0.006
134 49	HI	0.308	0.002	159 52	HI	1.438	0.007
135 49	HI	0.401	0.003	159 53	HI	1.456	0.007
136 49	HI	0.485	0.003	159 54	HI	1.441	0.008
137 49	HI	0.536	0.003	159 55	HI	1.429	0.006
138 49	HI	0.501	0.003	159 56	HI	1.426	0.006
139 49	FG	0.400	0.003	159 57	HI	1.402	0.006

TABLE 6.2. **(contd)**

Matrix	Loc[a]	$^{235}U(n,f)$[b]	σ	Matrix	Loc[b]	$^{235}U(n,f)$[b]	σ
140 49	FG	0.452	0.003	159 58	HI	1.354	0.006
141 49	FG	0.554	0.004	159 59	HI	1.292	0.006
142 49	CC	0.689	0.004	159 61	CC	1.155	0.005
143 49	HI	0.817	0.004	159 62	HI	1.049	0.005
144 49	CC	0.935	0.005	159 63	CC	0.955	0.005
145 49	HI	1.049	0.005	159 65	CC	0.694	0.004
146 49	CC	1.148	0.006	159 66	FG	0.559	0.003
147 49	HI	1.233	0.007	159 67	FG	0.449	0.003
148 49	HI	1.293	0.007	159 68	FG	0.393	0.003
149 49	HI	1.347	0.007	159 69	HI	0.484	0.004
150 49	HI	1.391	0.007	159 70	HI	0.515	0.004
151 49	HI	1.407	0.007	159 71	HI	0.475	0.003
152 49	HI	1.428	0.007	159 72	HI	0.392	0.003
153 49	HI	1.437	0.007	159 73	HI	0.299	0.002
154 49	HI	1.425	0.007	159 74	HI	0.218	0.002
155 49	HI	1.445	0.007	159 75	HI	0.148	0.002
156 49	HI	1.439	0.007	159 76	HI	0.081	0.001

[a]Drawer column which designates the foil location. Axial displacement from the reactor midplane was 63.1 mm.

[b]The data are given in units of 10^{-17} reactions/atom-watt-s. The uncertainties are one standard deviation as discussed in detail in the text.

TABLE 6.3. Basic Reaction Rate Data for Axial Distributions in ZPPR-15D

z,mm	Loc[a]	$^{239}Pu(n,f)$[b]	σ	$^{235}U(n,f)$[b]	σ	$^{238}U(n,f)$[b]	σ	$^{238}U(n,\gamma)$[b]	σ
		Traverse in Position 159 49							
77.0	HH	1.501	0.010	1.433	0.006	0.0354	0.0004	0.2031	0.0010
127.8	HH	1.451	0.010	1.388	0.006	0.0343	0.0004	0.1983	0.0010
178.6	HH	1.371	0.009	1.339	0.006	0.0331	0.0004	0.1886	0.0010
254.8	HH	1.246	0.009	1.196	0.006	0.0295	0.0004	0.1713	0.0008
331.0	HH	1.090	0.009	1.056	0.005	0.0255	0.0003	0.1504	0.0008
381.8	HH	0.954	0.008	0.928	0.005	0.0224	0.0003	0.1354	0.0007
432.6	HH	0.826	0.007	0.809	0.004	0.0172	0.0003	0.1189	0.0006
483.4	GH			0.699	0.004	0.0074	0.0002	0.0979	0.0005
534.2	GH			0.582	0.003	0.0038	0.0002	0.0836	0.0005
635.8	GH			0.387	0.003	0.0013	0.0001	0.0582	0.0004
737.4	GH			0.283	0.002	0.0006	0.0001	0.0421	0.0003
		Traverse in Position 159 60							
77.0	HI	1.337	0.009	1.217	0.005	0.0370	0.0004	0.1544	0.0008
127.8	HI	1.277	0.008	1.174	0.006	0.0359	0.0004	0.1497	0.0008
178.6	HI	1.234	0.010	1.122	0.005	0.0338	0.0004	0.1428	0.0007
254.8	HI	1.113	0.008	1.021	0.005	0.0311	0.0004	0.1294	0.0007
331.0	HI	0.952	0.008	0.881	0.004	0.0259	0.0003	0.1132	0.0006
381.8	HI	0.841	0.007	0.784	0.004	0.0216	0.0003	0.1014	0.0006
432.6	HI	0.700	0.006	0.665	0.004	0.0175	0.0003	0.0876	0.0005
483.4	GH			0.573	0.003	0.0080	0.0002	0.0782	0.0005
534.2	GH			0.477	0.003	0.0040	0.0002	0.0666	0.0004
635.8	GH			0.314	0.002	0.0012	0.0002	0.0462	0.0003
737.4	GH			0.221	0.002	0.0008	0.0001	0.0329	0.0002
		Traverse in Position 159 64							
77.0	HH	0.913	0.007	0.817	0.004	0.0318	0.0004	0.1036	0.0006
127.8	HH	0.879	0.007	0.783	0.004	0.0309	0.0004	0.1009	0.0005
178.6	HH	0.845	0.008	0.753	0.004	0.0289	0.0004	0.0958	0.0005
254.8	HH	0.745	0.007	0.674	0.003	0.0262	0.0003	0.0866	0.0005
331.0	HH	0.648	0.006	0.582	0.003	0.0221	0.0003	0.0752	0.0004
381.8	HH	0.565	0.006	0.515	0.003	0.0190	0.0003	0.0675	0.0004
432.6	HH	0.477	0.005	0.441	0.003	0.0150	0.0002	0.0589	0.0004
483.4	GH			0.371	0.002	0.0057	0.0002	0.0504	0.0003
534.2	GH			0.308	0.003	0.0029	0.0001	0.0437	0.0003
635.8	GH			0.203	0.002	0.0010	0.0001	0.0293	0.0002
737.4	GH			0.147	0.001	0.0008	0.0002	0.0220	0.0002

[a]Drawer column which designates the foil location. The ^{235}U foil was centered 13.84 mm above, the ^{238}U foil on, and the ^{239}Pu 13.84 mm below the mid-height of the drawer.

[b]The data are given in units of 10^{-17} reactions/atom-watt-s. The uncertainties are one standard deviation as discussed in detail in the text.

7. IN-CELL REACTION RATE MEASUREMENTS AND CELL FACTORS FOR ZPPR ASSEMBLY 15D (J. M. Gasidlo and D. W. Maddison)

Reaction rate maps are measured by placing single foils in matrix positions chosen to measure specific distributions such as a radial traverse along the x-axis or an axial traverse along the z-axis. Cell factors are used to convert the reaction rates measured in the mapping foils to reaction rates averaged over the materials used to construct the drawers.

Cell factors are obtained in special experiments where the ordinary plates used to build the reactor are replaced with special plates. The 6.35 mm thick plutonium fuel plates are replaced with two 3.175 mm plates and the 3.18 mm thick enriched uranium plates are replaced with two 1.59 mm plates. The 3.18 mm thick depleted uranium plates are replaced with special plates that have slots machined across the width of the plates. Here, special foils can be placed to measure the integral of the reaction rate across the width of the plate.

There are no half-thickness or slotted plates for the 1.59 mm thick enriched uranium plates or the 1.59 mm thick depleted uranium plates. The reaction-rate peaking in the 1.59 mm enriched urnaium plate was estimated to be -0.2% for ^{235}U fission, +3% for ^{238}U fission and -0.5% for ^{238}U capture which are one half the values measured for the 3.18 mm plate. The effect on the cell factors of these plate-peaking factors was 0.2% for ^{235}U fission 0.05% for ^{238}U fission and 0.01% for ^{238}U capture. The 1.59 mm depleted uranium plate was always adjacent to a 3.18 mm depleted uranium plate. The 3.18 mm plate was replaced with two 1.59 mm plates and reaction rates were measured between the plates. The plate-averaged value was taken the average of the two between-plate reaction rates. Using these two methods, "plate-averaged" reaction rates were determined for the plates from which the cell (drawer) was built. The process of generating cell factors from plate average reaction rates and mapping foil location rates is described in detail in Argonne National Laboratory report ANL-85-44.

The cell studies were performed on the y-axis. The drawers along the y-axis are mirrored so that a single-fuel-column-drawer will have an identical drawer on one side and various drawers on the other side. Along the x-axis single-fuel-column drawers alternate with double-fuel-column drawers. Since the cell factor for a drawer is affected by the drawer on either side (this is especially true at region boundaries such as the core/blanket interface), there may be different cell factors for a drawer on the y-axis compared to the same type of drawer on the x-axis. This is especially true for ZPPR-15D because the variation in the measured $^{238}U(n,f)$ rate across a single-fuel-column drawer with a 3.18 mm enriched uranium fuel plate is the greatest for any type of cell measured at ZPPR. The variations for $^{235}U(n,f)$ and $^{238}U(n,\gamma)$ are much smaller than for $^{238}U(n,f)$.

All of the data measured in the cell studies were used to derive cell factors for drawers on the y-axis. For single-fuel-column drawers on the x-axis, data from the cell studies were used only for that half of the drawer that was adjacent to a double-fuel column drawer. This is possible because the drawer is symmetrical. The cell factor for the double-fuel-column drawer was derived using the same method. The cell factors for $^{238}U(n,f)$ on the x- and y-axes differed by ~ 1%.

No cell studies were done for drawer masters 905 through 914. These masters have a single column of 1.59 mm-thick uranium fuel adjacent to a column of 3.18 mm-thick depleted uranium metal in the center of the drawer, which creates asymmetric in-cell reaction rate distributions. The cell factor was estimated for these drawers using data from other types of drawers. Cell-average reaction rates in these drawers should be considered as estimates only and should not be used to calculate core-average reaction rates.

The basic data for the cell studies are given in Table 7.1. The uncertainties given in the tables are due to counting statistics, foil positioning in the counter system and corrections for other isotopes in the foils.

The derived cell factors are given in Table 7.2. Under the heading "Environment" is listed the drawer master, the matrix positions, or the reactor region for which a cell factor is used. The key is DC for double-fuel-column drawer, RB for radial blanket, AB for axial blanket and RR for radial reflector. The mapping foil is in the center cell and is used for the given axial positions in mm. Note that the cell factors in the table for $^{239}Pu(n,f)$ and $^{235}U(n,f)$ in the radial and axial blankets are given as unity. As foil positions in the radial and axial blankets (and the radial reflector) get farther from the core boundary, self-shielding in the irradiation foil becomes very important. This self-shielding can be from ~ 1% near the core to > 5% at the blanket boundaries and in the reflector. Hence, cross sections self-shielded especially for the irradiation foils must be used in these regions. Note that for ^{238}U in the axial and radial blankets, the plate-averaging foils are self-shielded by the blanket materials. Hence, the use of cell factors for ^{238}U is valid in the blanket regions.

The uncertainties given in the table are solely those due to counting statistics and data reduction. They are random for the determination of a single cell factor, but they are systematic when applied to the cell-averaged reaction rate distributions. Additional systematic uncertainties which are not included are described in the Argonne National Laboratory report ANL-85-44.

TABLE 7.1. Basic Reaction Rate Data for Cell Factor Studies in ZPPR-15D

Matrix	Loc[a]	$^{235}U(n,f)$[b]	σ	$^{238}U(n,f)$[b]	σ	$^{238}U(n,\gamma)$[b]	σ
144 49	-PP			0.0277	0.0002	0.1111	0.0005
144 49	CD	0.880	0.003	0.0327	0.0002	0.1156	0.0005
144 49	HH	0.874	0.004	0.0276	0.0002	0.1150	0.0005
144 49	-HI			0.0270	0.0002	0.1114	0.0005
144 49	MN	0.876	0.003	0.0320	0.0002	0.1159	0.0005
144 49	-AA			0.0292	0.0002	0.1100	0.0005
146 49	-AA			0.0332	0.0002	0.1339	0.0006
146 49	CD	1.075	0.004	0.0382	0.0002	0.1422	0.0006
146 49	HH	1.070	0.004	0.0317	0.0002	0.1406	0.0006
146 49	-HI			0.0314	0.0002	0.1353	0.0006
146 49	MN	1.069	0.004	0.0380	0.0002	0.1415	0.0006
146 49	-PP			0.0338	0.0002	0.1328	0.0006
250 48	NN	1.301	0.005	0.0325	0.0002	0.1634	0.0007
250 48	MN	1.306	0.005	0.0338	0.0002	0.1733	0.0007
150 48	HH	1.306	0.005	0.0441	0.0003	0.1740	0.0007
150 48	HI	1.303	0.005	0.0488	0.0003	0.1710	0.0007
150 48	II	1.302	0.005	0.0442	0.0002	0.1738	0.0007
250 48	CD	1.312	0.005	0.0347	0.0002	0.1721	0.0008
250 48	CC	1.300	0.005	0.0339	0.0002	0.1632	0.0007
245 49	NN	0.982	0.004	0.0306	0.0002	0.1233	0.0005
245 49	MN	0.986	0.004	0.0306	0.0002	0.1287	0.0006
145 49	HH	0.976	0.004	0.0405	0.0002	0.1303	0.0006
145 49	HI	0.998	0.004	0.0432	0.0003	0.1287	0.0005
145 49	II	0.994	0.004	0.0398	0.0002	0.1293	0.0005
245 49	CD	0.982	0.004	0.0322	0.0002	0.1284	0.0005
245 49	CC	0.982	0.004	0.0315	0.0002	0.1229	0.0005

TABLE 7.1. (contd)

Matrix	Loc[a]	$^{235}U(n,f)$[b]	σ	$^{238}U(n,f)$[b]	σ	$^{238}U(n,\gamma)$[b]	σ
243 49	NN	0.752	0.003	0.0229	0.0002	0.0968	0.0004
243 49	MN	0.749	0.003	0.0230	0.0002	0.1009	0.0004
143 49	HH	0.758	0.003	0.0308	0.0002	0.1021	0.0004
143 49	HI	0.753	0.003	0.0334	0.0002	0.1005	0.0004
243 49	CD	0.754	0.003	0.0235	0.0002	0.1011	0.0004
243 49	CC	0.751	0.003	0.0232	0.0002	0.0962	0.0004
Data Near the Core-axial Blanket Interface							
243 49	NN	0.418	0.002	0.0106	0.0001	0.0553	0.0003
243 49	MN	0.419	0.002	0.0105	0.0001	0.0585	0.0003
143 49	HH	0.418	0.002	0.0148	0.0001	0.0590	0.0003
143 49	HI	0.415	0.002	0.0160	0.0001	0.0578	0.0003
143 49	II	0.416	0.002	0.0146	0.0001	0.0589	0.0003
243 49	CD	0.420	0.002	0.0109	0.0001	0.0582	0.0003
243 49	CC	0.417	0.002	0.0107	0.0001	0.0549	0.0003

[a]Drawer column which designates the foil location. Axial displacement was 63.1 mm for ^{235}U and 77.0 mm for ^{238}U foils.

[b]The data are given in units of 10^{-17} reactions per atom-watt-s. The uncertainties are one standard deviation as discussed in detail in the text.

TABLE 7.2. Cell Factors for the Reference Map of ZPPR-15D

$^{239}Pu(n,f)$[a]	σ	$^{235}U(n,f)$[a]	σ	$^{238}U(n,f)$[a]	σ	$^{238}U(n,\gamma)$	σ	Environment[b]	z,mm[c]
1.0	0.01	1.0000	0.0048	0.7846	0.0114	0.8954	0.0053	901-904	0-381.8
1.0	0.01	1.0000	0.0070	0.8717	0.0182	0.9745	0.0130	905-914	0-381.8
1.0	0.01	0.9990	0.0048	0.7465	0.0127	0.9319	0.0057	915-920	0-381.8
1.0	0.01	0.9984	0.0045	0.7742	0.0077	0.9502	0.0051	158-62,64	0-381.8
1.0	0.01	1.0000	0.0040	0.8694	0.0080	0.9482	0.0060	158-61,63,65	0-381.8
1.0	0.01	0.9984	0.0045	0.7628	0.0082	0.9502	0.0051	143,145-49	0-381.8
1.0	0.01	1.0000	0.0040	0.8613	0.0064	0.9482	0.0060	142,144,146-49	0-381.8
1.0	0.008	1.0	0.008	1.029	0.025	1.0119	0.0060	DC-RB-RB	ALL
1.0	0.008	1.0	0.008	1.029	0.025	1.0178	0.0042	RB-RB-RB	ALL
1.0	0.008	1.0	0.008	1.029	0.025	1.0279	0.0043	RB-RB-RR	ALL
1.0	0.01	1.0000	0.0083	0.7504	0.0154	0.8823	0.0086	901-904	432.6
1.0	0.01	1.0000	0.0090	0.8376	0.0182	0.9583	0.0143	905-914	432.6
1.0	0.01	0.9980	0.0051	0.7247	0.0083	0.9363	0.0053	923-924,927-928	432.6
1.0	0.01	1.0	0.01	0.923	0.037	0.8979	0.0054	AB	483.4
1.0	0.01	1.0	0.01	0.950	0.059	0.8778	0.0055	AB	534.2
1.0	0.01	1.0	0.01	1.004	0.031	0.8641	0.0036	AB	635.8
1.0	0.01	1.0	0.01	1.06	0.14	0.7982	0.0076	AB	737.4

[a]Uncertainties are due to counting statistics and data reduction only. See the test for details on other uncertainties.

[b]The mapping foil is in the center cell. See the text for the key to the abbreviations.

[c]Axial distance from the reactor midplane for which the cell factor can be used.

8. MESUREMENT AND ANALYSIS OF CONTROL ROD WORTHS IN ZPPR-15D

(D. M. Smith and P. J. Collins)

Control rod worths were measured in ZPPR-15D for the primary and secondary rod banks, for the primary rod bank with one and two rods missing and for a special segmented control rod design at the core center. All measurements were made relative to fuel since the 15D reference core did not contain control rod positions (CRPs).

The locations of the control rods, Fig. 8.1, were the same as in the plutonium fuelled core, ZPPR-15B (ZPR-TM-472, p. 3). Rods 1 and 8 through 13 are designated as primary rods and rods 2 through 7 are designated secondary rods. All control rods were four ZPPR drawers in size (110 mm x 110 mm) and were composed of 50% natural B_4C plates and 50% sodium plates by volume. The boron section of the rods extended over the core height (914 mm) and the remainder of the drawers (follower section of the rods) contained sodium plates.

A special measurement of a "segmented" control rod design was made at the center of ZPPR-15D. This rod contained alternating sections of 100% volume fraction natural B_4C (three 203 mm sections) and steel (two 152 mm sections), the steel sections representing links in the rod to enable it to be inserted in a distorted channel. The drawer master for this rod design is shown in Fig. 8.2. The aim of this measurement was to compare the worth predictions, using standard analysis methods, with those for rods uniformly loaded with B_4C. The worth of a reference rod, fully loaded with B_4C, shown in Fig. 8.3, was also measured for comparison.

The control rod worths were measured in a variant of the ZPPR-15D subcritical reference (ZPR-TM-471, p. 17). Modifications to this configuration were only the movement of two in-core fission chambers, numbers 16 and 52, away from control rod locations. The rod bank measurements were made in loadings 193 to 200, reactor runs 326 to 333, between June 6, 1986, and June 12, 1986. The reference reactivity for these measurements was -7.55 ¢ ± 0.054¢, measured by inverse kinetics analysis of a rod drop in loading 193 , reactor run 326. The segmented

rod and its "solid B_4C" reference rod were measured a little later in the program, in loading 208 to 210, reactor runs 369 and 371, between July 25, 1986, and July 28, 1986. A new reference was established for these measurements in loading 208, reactor run 369, with reactivity $-4.036¢ \pm 0.018¢$.

Compositions for the segmented rod and its partner are given in Table 8.1. Compositions for the 50% B_4C plate rod used in the bank measurements are given in ZPR-TM-472, Table 2.1.

Details of the modified-source-multiplication method used to determine the control rod worths are given in ZPR-TM-442, p. 7. The "detector efficiencies" and "effective source ratios" input to the McCRUNCH code were calculated by two-dimensional (xy) diffusion theory with twenty-one energy groups and a constant buckling. All measured worths were taken from the least-squares fit analysis in the McCRUNCH code. Minor improvements to initially calculated source ratios were included in the McCRUNCH processing. The data processing and measured rod worths are shown in Table 8.2.

Calculated control rod worths were obtained with the xyz model of ZPPR-15D using a nodal diffusion theory solution and the ENDF/B-V.2 data in 21 energy groups. The calculation model and details of cross section processing are described in Section 3 of this report. Cross sections for boron in the control rods were used at infinite dilution and collapsed to 21 groups with the 230 group core spectrum from the cylindrial diffusion model. This treatment follows the IFR design method. For the segmented rod, the axial node boundaries were changed from those in the reference model (Section 3) to match the boron and steel zones of the rod at 102 mm and 255 mm. The materials between 407 mm and 466 mm were reduced in density to match the uranium fuel height (Section 3).

The calculated control rod worths are given in Table 8.3. Rod worths are defined as $(k_1 - k_2)/k_1k_2\beta$, with k_1 the k-effective of the reference, k_2 the k-effective rods with inserted and $\beta = 0.6527\%$ (Section 4). The

worths obtained by finite-difference diffusion, as a by-product of the data processing, are also shown in Table 8.3.

The calculated and measured control rod worths are compared in Table 8.4. The worths are about a factor of two smaller than in the plutonium core ZPPR-15B due to the increased delayed neutron fraction. The C/E ratio for the primary rods are quite consistent varying from 0.963 at the center to 0.966 for the banks of 6 or 7 rods. The uniform prediction as a function of radius is consistent with the reaction rate analysis (Section 5). In contrast, the corresponding C/E results for rod worths in ZPPR-15B varied from 1.018 at the center to 0.980 for the 7 primary rods. Because of the consistency in prediction for banks of 5, 6 and 7 primary rods, the worths of rods missing from the bank (rod run-out effects) are consistently calculated.

The worth of all 13 rods (C/E = 0.991) is predicted 2.5% higher than for the primary rods alone, implying an overprediction of 5% for the six secondary rods relative to the primary rods. This discrepancy appears to be associated with calculations involving the drawers with 1/8 in. thick uranium fuel. Drawers with thick fuel were replaced by secondary rods but not by primary rods. The ^{235}U fission rates in drawers with thick fuel were underpredicted by 2% to 3% relative to neighboring locations (Section 5). Thus, the discrepancies in prediction of the secondary rods appears to be due to inadequate treatment of these cells in the cross section processing.

The segmented control rod is predicted consistently with the solid B_4C rod. The C/E ratios for these rods are 2.5% higher than for the 50% B_4C rod. A similar result was found in nodal diffusion analysis for ZPPR-15B (ZPR-TM-472, Table 2.4.). Calculations with an rz model for ZPPR-15B showed that this difference can be largely accounted for by transport corrections.

TABLE 8.1. Atom Densities for the Segmented Control Rod in ZPPR-15D (atoms/barn-cm)

	Master 628[a]				Master 629[a]
Isotope	0 - 4	4 - 10	10 - 18	18 - 36	4 - 10
B-10	0.0141613	---	0.0143606	---	0.0143373
B-11	0.0574157	---	0.0582273	---	0.0581427
C	0.0185753	0.0001124	0.0188371	0.0001163	0.0188112
O	---	0.0000007	---	0.0000007	---
Na	---	0.0101800	---	0.0101800	---
Si	0.0002179	0.0004566	0.0002157	0.0004585	0.0002180
Al	0.0000029	0.0000061	0.0000043	0.0000061	0.0000038
Mn	0.0002467	0.0007082	0.0002443	0.0007108	0.0002458
Cr	0.0029702	0.0083994	0.0029125	0.0084290	0.0029319
Fe	0.0106022	0.0294087	0.0104122	0.0295918	0.0104797
Ni	0.0013291	0.0036052	0.0012953	0.0036173	0.0013054
Cu	0.0000291	0.0000622	0.0000297	0.0000626	0.0000297
Mo	0.0000151	0.0000562	0.0000143	0.0000564	0.0000145

[a]Compositions are given for axial segments of the control rods, labelled to the nearest inch for brevity. Compositions for Master 629 are the same as for Master 628 except in the range 4.036 in. to 10.036 in.

TABLE 8.2. Measured Control Rod Worths in ZPPR-15D

Configuration	Data File	No. of Detectors	Input Source Ratio	Worth, $[a]	σ_s, %[b]	σ_t, %[b]
Central CRP	182	62	1.0044	0.158	0.205	0.868
Central CR (50% B_4C)	183	59	1.0210	1.389	0.205	0.806
5 Primary CRs (11,13 missing)	185	50	0.9818	6.160	0.304	0.835
6 Primary CRs (13 missing)	184	50	1.0026	7.715	0.323	0.841
7 Primary CRs	186	46	1.0242	9.580	0.382	0.867
All 13 CRs	187	40	1.0693	19.139	0.561	0.961
Repeat Reference	188	62	1.000	-0.0009	---	---
Central CR (100% B_4C)	196	55	1.0297	1.946	0.156	0.560
Central CR[c] (Segmented)	195	59	1.0297	1.397	0.194	0.577

[a] First seven worths relative to reference ρ = 7.55¢, data file 179. Last two worths relative to reference ρ = 4.04¢, data file 194.

[b] σ_s is the total statistical uncertainty including contributions from the least-squares fitting, corrections to temperature, interface separation and ^{241}Pu decay. σ_t is the total uncertainty including correlated components for reactivity calibration and relative source ratios.

[c] Using efficiencies and initial source ratios calculated for the 100% B_4C rod.

TABLE 8.3. Calculations of Control Rod Worths in ZPPR-15D

Case	k-effective[a]	Worth, $	FDDT[b] Worth, $
Reference	0.990073	---	---
Central CRP	0.988881	0.186	0.221
Central 50% B_4C	0.981591	1.337	1.265
5 Primary CRs	0.953476	5.940	5.771
6 Primary CRs	0.944560	7.456	7.196
7 Primary CRs	0.934192	9.257	8.918
All 13 CRs	0.881950	18.971	18.256
Central 100% B_4C	0.977878	1.930	1.825
Central Segmented Homogenized Segmented CR	0.981256	1.390	---
	0.980073	1.579	---

[a]Calculation xyz nodal diffusion with 21 energy groups βeff = 0.6527%.

[b]Finite difference calculations xy geometry used for data processing. Reference k-effective = 0.993429.

TABLE 8.4. Comparison of Calculated and Measured Control Rod Worths in ZPPR-15D

Rods	Experiment, $	Calculation, $	C/E	C/E in ZPPR-15B
Central CRP	0.158	0.186	1.18	1.17
Central CR	1.389	1.337	0.963	1.018
5 Primary	6.160	5.940	0.964	0.965
6 Primary	7.715	7.456	0.966	---
7 Primary	9.580	9.257	0.966	0.980
All 13 CRs	19.139	18.971	0.991	0.953
Central 100% B_4C	1.946	1.930	0.992	1.043
Central Segmented	1.397	1.390	0.995	---

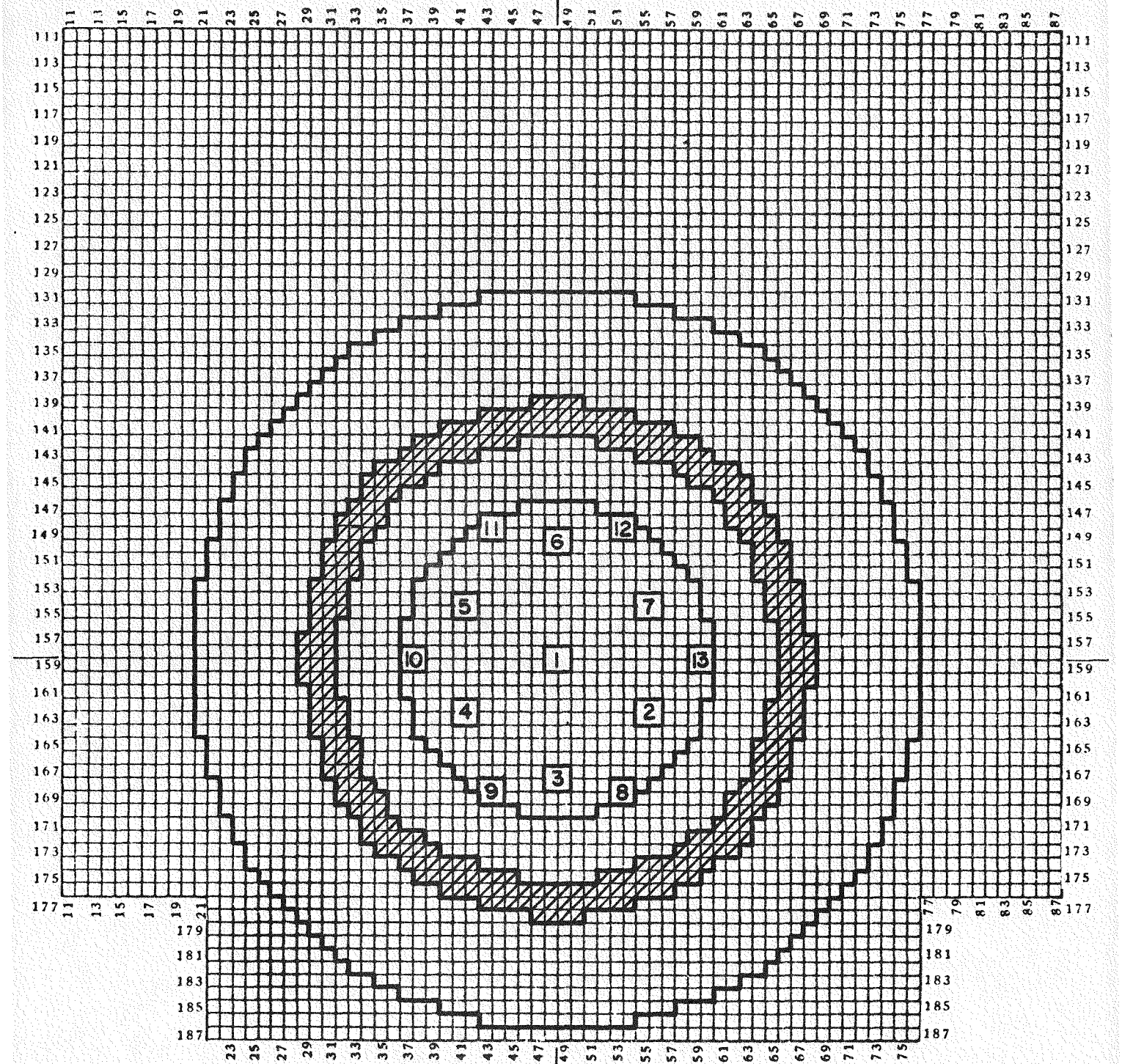

Fig. 8.1. Control Rod Locations and Numbering Scheme in ZPPR-15D.

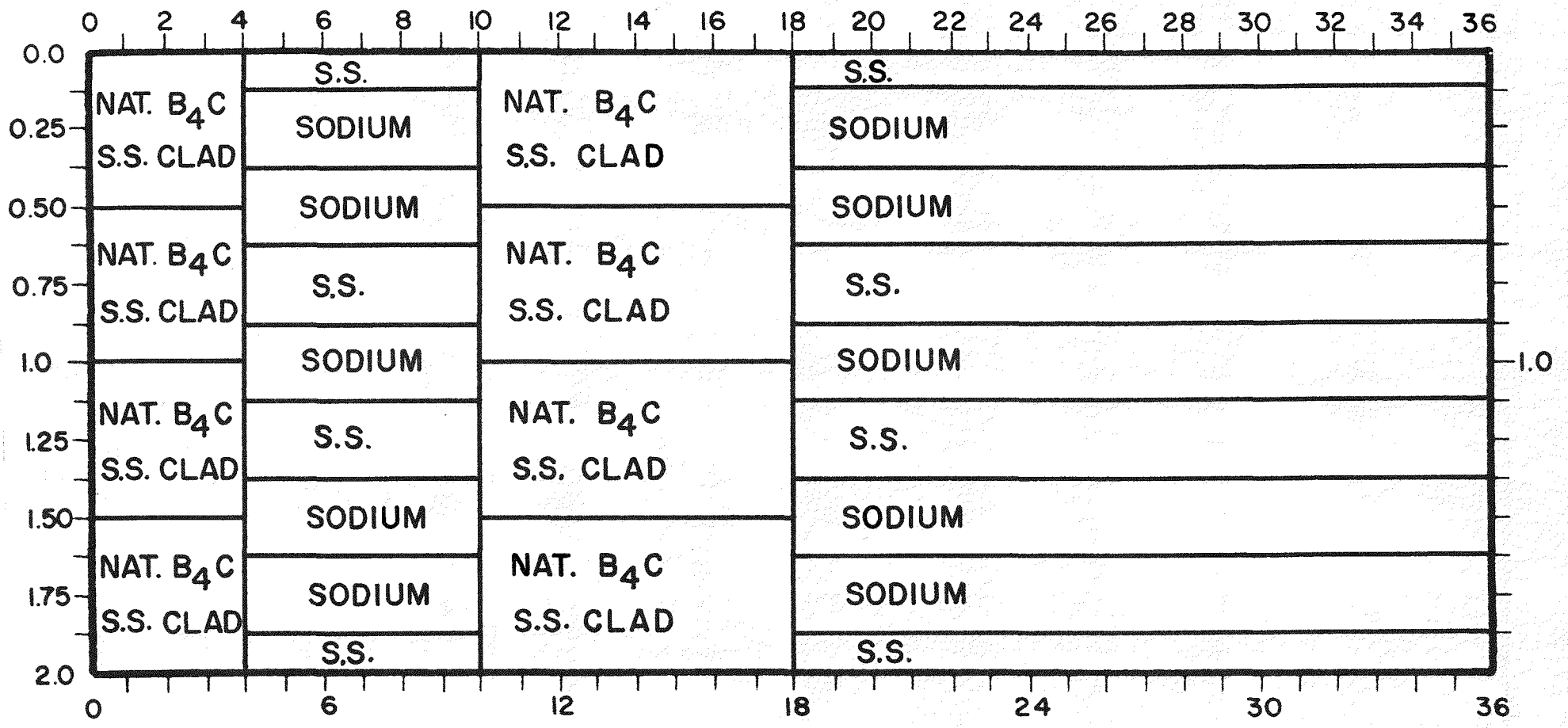

Fig. 8.2. Segmented Control Rod in ZPPR-15D.

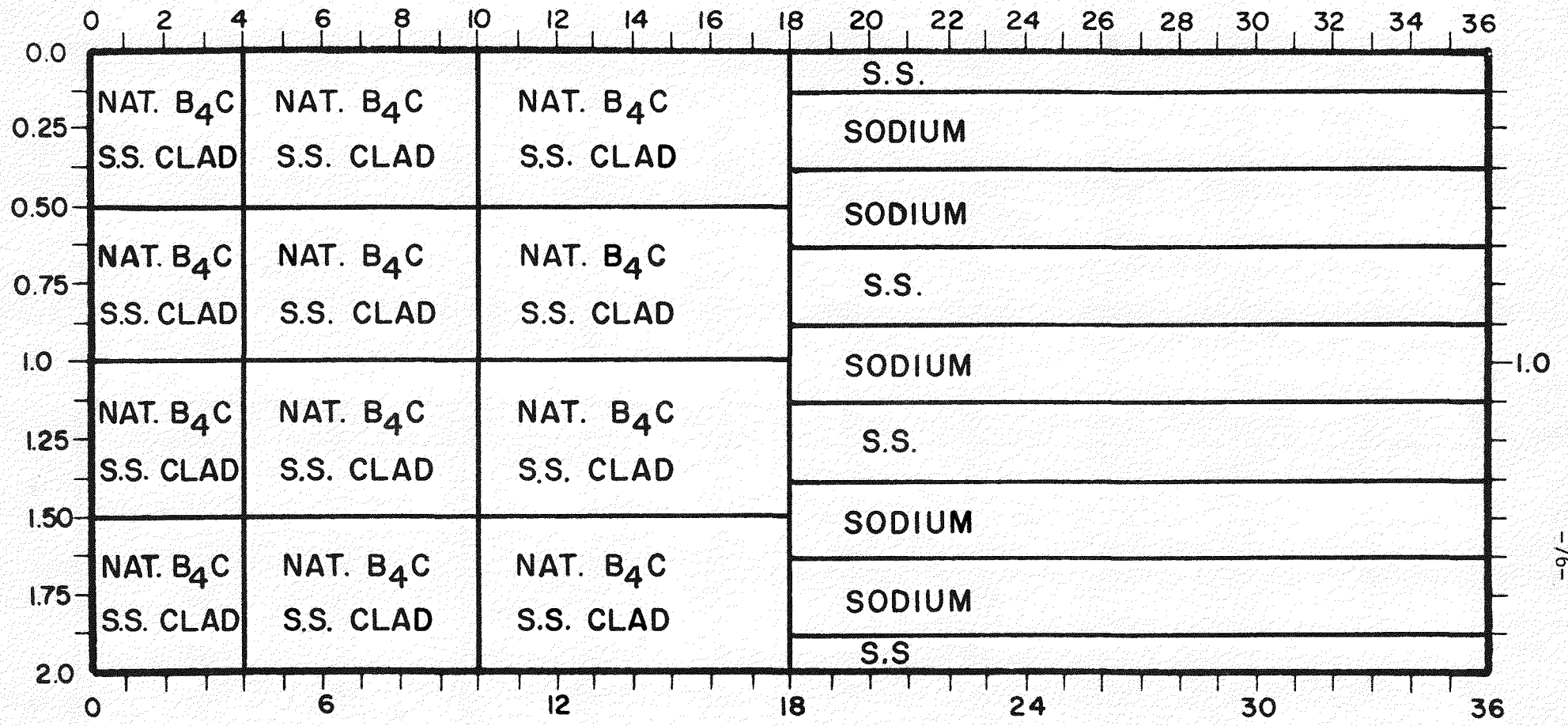

Fig. 8.3. 100% B_4C Control Rod in ZPPR-15D.

9. SODIUM VOID MEASUREMENTS AND ANALYSIS IN ZPPR-15D (S. B. Brumbach, R. E. Kaiser and G. L. Grasseschi)

Reactivity changes due to sodium voiding were measured in two axial steps in the central 52 drawers in each assembly half of the "symmetric-zirconium" zone of ZPPR-15D. The measurements were made by replacing sodium-filled cans with empty cans. The reactivities were measured by subcritical source multiplication using the countrates from 63 fission chambers relative to countrates in a reference configuration whose reactivity was calibrated by inverse kinetics analysis of the power history following a rod drop.

The subcritical reference for ZPPR-15D (reactor loading 184) was established initially on May 23, 1986. This configuration was described in ZPR-TM-471, p. 17. Because the worth of sodium removal was expected to be small in the all-uranium-fuel zone in ZPPR-15D, the subcritical reference was used as the starting point for the sodium void measurements. The sodium voiding steps, ±203 mm and ±457 mm, were made in the central 52 drawers of each assembly half in reactor loadings 189 and 190. The sodium was added back in a reflood step in loading 191. All drawers in the void zone contained a single column of 1.59 mm-thick uranium fuel. Two drawers with fission chambers (master 735) were in the void zone and were voided along with the other drawers (voided masters 744 and 745).

The experiments were conducted between May 30, 1986 and June 4, 1986 in reactor runs 321 to 323. The fission chamber data were recorded on data files 176 to 178. The reactivity calibration was made in the subcritical reference loading in run 312 (fission chamber data file 171), inverse kinetics data file 1). The reactivity of this reference was -7.075 ± 0.059 ¢. The reactivity of the void steps were determined relative to this reference by analysis of the fission chamber countrates with the McCRUNCH code. One detector (number 41) out of the 64 and 2 thermocouples (numbers 1 and 76) out of the 16 were inoperative during the measurements and were excluded from the analysis. Detector efficiency ratios and effective source ratios of unity were assumed in the data

processing with detectors predicting reactivities more than 3.6 standard deviations from the mean being rejected. At least 57 out of the 63 detectors were retained by this process.

The reactivity analysis results from the McCRUNCH code are summarized in Table 9.1. Reactivities are relative to the subcritical reference. The statistical uncertainties shown result from the detector countrates and from corrections for temperature, interface gap and ^{241}Pu decay (The core contained about 10% Pu fuel). The correlated uncertainties are due to reactivity scale calibration and source ratio. Because the reflood step brought the assembly back to the subcritical reference, the expected reactivity after reflood is zero. The measured reactivity was 0.13¢. This discrepancy is attributed to movement of plates in the drawers during the voiding operation. Since the precise origin of the reactivity increment is unknown, we attribute an additional 1σ uncertainy of 0.13¢ to each void step reactivity.

The reactivities of the void steps are given in Table 9.2. In the measurements, the mass of steel changed slightly with each void step due to differences in masses of sodium cans and empty cans. Corrections for the steel changes, given in the table, were taken from calculations for ZPPR-15A and an uncertainty of 30% of the correction was included in the statistical uncertainty for each step.

Calculations of sodium void reactivity were made by direct k-differences using the xyz model of ZPPR-15D with nodal diffusion solutions in 21 groups. Cross sections for the void cell were processed for heterogeneity with the SDX code and collapsed from 230 groups to 21 groups in a one-dimensional reactor model. Data for the remainder of the central symmetric-zirconium zone surrounding the void zone were also generated in this model. Anisotropic diffusion coefficients were generated for the voided cell by the Benoist method. Compositions of the fission chamber drawers were not included in the calculation model and these were treated as normal fuel drawers. Differences in sodium content are allowed for by using the reactivity per mass of sodium for comparison with experiment. Details of the cross section processing and reactor

model are given in Section 3. Calculated reactivities in dollars were defined by $\Delta k/(k_1 k_2 \beta)$ with a value of 0.006564 for the effective delayed neutron fraction β (Section 4).

The calculated void reactivities are compared with measurement in Table 9.3. The central sodium void reactivity (0-233 mm) in ZPPR-15D of 0.233 ¢/kg(Na) is small compared with the measurement in the plutonium fuelled core ZPPR-15B. The corresponding void reactivity in that case was 2.083 ¢/kg(Na). Note that the value for β is about a factor of two higher in the uranium core. The discrepancies in calculation are large in relation to the measured void reactivities in 15D but are of a similar absolute magnitude to those observed in the ZPPR-15B analysis (ZPR-TM-471 p.34).

TABLE 9.1. Data Processing for ZPPR-15D Sodium Void Experiments

Measurement	Data File	No. of Detectors[b]	χ^2[c]	Reactivity, ¢[a]	σ_s,¢[d]	σ_c,¢[e]
203 mm Void	176	59	1.093	4.79	0.04	0.04
457 mm Void	177	57	1.420	-0.65	0.01	0.01
Reflood	178	62	1.098	0.13	0.02	0.01

[a]Reactivities are derived relative to the subcritical reference for which detector counts are recorded on File 171. The reactivity of this configuration was determined by inverse kinetics (File 1) to be -7.075 ± 0.059 ¢.

[b]Number of detectors remaining after rejection of those giving reactivities which were more than 3.6 standard deviations from the mean.

[c]Value of chi-square for remaining detectors using counter statistics.

[d]Statistical uncertainty.

[e]Correlated uncertainty.

TABLE 9.2. Experimental Reactivity Changes for Sodium Void Steps in ZPPR-15D

Step[a]	Mass Sodium Voided, kg	Mass Steel Added, kg	Measured Reactivity Change, ¢	Steel Correction, ¢	Corrected Reactivity, ¢	σ_s,¢[d]	σ_c,¢[d]	Specific Reactivity ¢/kg (Na)
0-203 mm	20.804	0.366	4.79	+0.06	4.85	0.04	0.04	0.233
0-457 mm	46.080	2.395	-0.65	+0.26	-0.39	0.04	0.04	-0.008
203-457 mm	25.276	2.029	-5.44	+0.20	-5.24	0.06	0.06	-0.207

[a]Voiding symmetrically in each half of the matrix.

[b]Statistical uncertainty including 30% of the steel correction, but not including reproducibility uncertainty (0.13¢).

[c]Correlated uncertainty includes reference reactivity and source ratio uncertainties.

TABLE 9.3. **Calculated Reactivities for Sodium Voiding in ZPPR-15D and Comparison with Experiment**

Step[a]	Calculated k_{eff}	Calculated Worth, ¢[c]	Mass Sodium Voided, kg	Specific Reactivity ¢/kg (Na)	C-E ¢/kg (Na)	Experimental Uncertainty[d] ¢/kg (Na)
0-203 mm	0.990608	+7.16	20.568	+0.3489	+0.115	0.0068
0-457 mm	0.990352	+3.18	47.128	+0.0675	-0.076	0.0031
203-457 mm	---	-3.98	26.560	-0.1498	-0.057	-0.0061

[a]Voiding symmetrically in each reactor half.

[b]Nodal diffusion calcultion, 21 groups.

[c]Using βeff = 0.006564.

[d]Experimental uncertainty includes reproducibility.

10. GAMMA RAY DOSE DISTRIBUTION IN THE ZPPR-15B CORE AND SHIELDING EXPERIMENTS (D. N. Olsen and T. S. Huntsman)

The gamma ray dose distribution was measured along the x and y axes of the ZPPR-15B critical reference (ZPR-TM-470, p. 3) and through the two ZPPR-15B shield zones (ZPR-TM-472, p. 17). In addition, the gamma dose distribution was measured through the four ZPPR-15B fuel cells to provide data on the in-cell distributions. Stainless-steel-encapsulated ^{7}LiF thermoluminescent dosimeters (TLDs) were used.

Two types of dosimeters were employed for the irradiations. The first was a stainless-steel cylinder of 12.7 mm diameter and 6.4 mm height which can contain up to five TLDs. These dosimeters are loaded into special tunnel sodium plates which replaced normal sodium within the cell. Dosimeters of this type were used in the core, blanket and most of the locations of the two shield zones.

The second type of dosimeter was a stainless-steel cylinder of 3.2 mm diameter and 12.7 mm height which contains one TLD. This type of dosimeter was positioned in slots milled into the top of the steel reflector blocks or sandwiched between the plates of materials for the in-cell gamma distribution measurements.

All irradiations were performed such that the integrated power was about 300 watt-hours. Integrated counts from the ex-core BF_3 chambers provided power normalization. Thus, the TLD dose measurements can be accurately normalized to the reactor fission rates measured in foil irradiations. The reported dose is the dose rate at an estimated power of one watt. The dosimeters were removed from the assembly 20 hours after reactor shutdown.

TLDs are sensitive to neutrons and gamma rays. The neutron contribution is approximately 20% of the measured dose and is a function of position. The neutron and gamma contributions can be separated by calculation of the two fluxes, but the values reported are the total dose

rate. The dose rates are given in millirads per second (mrd/s) where 1 rd = 0.01 Gy in SI units.

The dose rate (neutron plus gamma) measured in the xy mapping of the ZPPR-15B reference configuration is given in Table 10.1. The dosimeters contained two TLDs and the reported dose rate is the average. All dosimeters were located 76.2 mm behind the half 1 interface. The intracell TLD locations are given in the footnotes of Table 10.1 for the various cell types and are shown for the fuel drawers as "TLD" in the cell drawings in Fig. 10.1.

The dose rate (neutron plus gamma) through the outer core, blanket, shields of the two shield zone configurations and the reference are given in Table 10.2. All dosimeters were located 76.2 mm behind the half 1 interface. The intracell location in the shield zone was at the center of the matrix position.

For comparison, the dose rate (neutron plus gamma) in the x axis positions symmetric to the shield zone are given in Table 10.3. The intracell locations are reflected so they are equivalent to the reference locations shown in Fig. 10.1.

The dose in the TLD is not the average dose in the cell. The dose distribution in the 15B cells was measured to establish the relationship between dose at the TLD location and other locations in the cell. This relationship is needed when comparing doses measured in different cell types. Measurements were made in fuel cells located along the y-axis to minimize radial gradients across the cell. The TLDs were sandwiched between the materials of the cell for the irradiation.

The cell structure results are shown in Fig. 10.1. The dose is normalized to 1.0 at the largest experimental value in each cell. The in-cell distribution is nearly the same for the two single-fuel-column cell types. The outer core measurement was made as a two cell unit because the fine structure is dependent upon the neighboring cells and because the two-unit cell is the most common in the outer core. As one would expect

from the sources of the gammas, the dose rate in the dosimeter is high near the fuel, peaking by as much as 40% and depressed near the heavy metal. The other materials of the cell have only minor effect compared to the fissile-containing plates.

TABLE 10.1. Dose Rate (Gamma and Neutron) in Stainless Steel Encapsulated ^{7}LiF TLDs along the x and y Axes of the Reference Configuration of ZPPR-15B

x-axis		y-axis			
Matrix Location	Dose Rate[a] (mrd/s)	Matrix Location	Dose Rate[a] (mrd/s)	Region	Cell[b] Type
159-48	0.6843	158-48	0.6926		SCS
159-47	0.6855	157-48	0.6971		SCS
159-46	0.6897	156-48	0.7034		SCS
159-45	0.6924	155-48	0.6893		SCS
159-44	0.6728	154-48	0.7017		SCS
159-43	0.7038	153-48	0.6883	Inner Core	SCS
159-42	0.6867	152-48	0.7005		SCS
159-41	0.6690	151-48	0.6752		SCA
159-40	0.6631	150-48	0.6622		SCA
159-39	0.6565	149-48	0.6581		SCA
159-38	0.6339	148-48	0.6534		SCA
159-37	0.6528	147-48	0.6530		SCA
159-36	0.6334	146-48	0.6184		DC
159-35	0.6181	145-48	0.6052	Outer Core	SC
159-34	0.5377	144-49	0.5283		DC
159-33	0.4876	143-48	0.4777		SC
159-32	0.3821	142-48	0.3623		DC
159-31	0.1587	141-48	0.1609		
159-30	0.0948	140-48	0.0976	Blanket	Blanket
159-29	0.0665	139-48	0.0694		
159-28	0.0419				
159-26	0.0316			Reflector	
159-24	0.0198				
159-22	0.0094				

[a]Estimated reactor power of 1 watt. Statistical uncertainty 2%. All TLDs are located 76.2 mm behind the reactor interface. The intracell locations are: Core - Columns JK, Blanket and Reflector - Columns HI. (See Fig. 10.1) The intracell location is specified by dividing the drawers into 16-1/8 in.-wide columns. Each column is assigned a letter with A at the left as one faces the drawer. The TLD spans the columns indicated by the letters.

[b]SCS = Symmetric single-fuel-column, SCA = Asymmetric single-fuel-column, DC = Double-fuel-column, SC = Single-fuel-column.

TABLE 10.2. Dose Rate (Gamma and Neutron) in Stainless Steel Encapsulated ^{7}LiF TLDs through the ZPPR-15B Shield Zones

Matrix Location[a]	Region	Configuration: Reference Dose Rate[a] (mrd/s)	Reference Cell Type[b]	Shield 1 Dose Rate[a] (mrd/s)	Shield 1 Cell Type[b]	Shield 2 Dose Rate[a] (mrd/s)	Shield 2 Cell Type[b]
159-36		0.6334	DC	0.6285	DC	0.6429	DC
159-35		0.6181	SC	0.6163	SC	0.6321	SC
159-34	Outer Core	0.5377	DC	0.5056	DC	0.5155	DC
159-33		0.4876	SC	0.4578	SC	0.4862	SC
159-32		0.3821	DC	0.3536	DC	0.3578	DC
159-31		0.1587		0.1539		0.1531	
159-30	Blanket	0.0948	Blanket	0.0950	Blanket	0.0942	Blanket
159-29		0.0665		0.0673		0.0634	
159-28		0.0419	SS	0.0428	SSNA	0.0356	SSNA
159-27				0.0366	SSNA	0.0257	SSNA
159-26		0.0316	SS	0.0313	SSNA	0.0156	SSNA
159-25				0.0258	SSNA	0.0139	BCNA
159-24		0.0198	SS	0.0199	SSNA	0.0082	BCNA
159-23				0.0152	SSNA	0.0044	BCNA
159-22		0.0094	SS	0.0110	SSNA	0.0024	BCNA
159-21	Shield Zone			0.0069	SSNA	0.0014	BCNA
159-20				0.0044	SP	0.0008	SP
159-19				0.0034	SP	0.0005	SP
159-18				0.0025	SP	0.0004	SP
159-17				0.0020	SP	0.0003	SP
159-16				0.0016	BCNA	0.0003	BCNA
159-15							
159-14				0.0006	MS	0.0002	MS
159-13							
159-12				0.0003	MS	0.0001	MS

[a]Estimated reactor power of 1 watt. Statistical uncertainty 2%. All TLDs are located 76.2 mm behind the reactor interface. The intracell locations are: Core - Columns JK, Blanket and Shield Zone - Columns HI. The intracell location is specified by dividing the drawers into 16-1/8 in.-wide columns. Each column is assigned a letter with A at the left as one faces the drawer. The TLD spans the columns indicated by the letters.

[b]SC = Single-fuel-column, DC = Double-fuel-column, SSNA = Sodium/stainless-steel, BCNA = B_4C/sodium, SP = sodium pool, MS = Mild Steel, SS = Stainless Steel

TABLE 10.3. Dose Rate (Gamma and Neutron) in Stainless Steel Encapsulated ^{7}LiF TLDs through the Normal Reflector of the Shield Zone Configurations of ZPPR-15B

Matrix Location[a]	Region	Configuration: Shield 1 Dose Rate[a] (mrd/s)	Configuration: Shield 2 Dose Rate[a] (mrd/s)	Cell Type[b]
159-61		0.6370	0.6603	DC
159-62		0.6313	0.6265	SC
159-63	Outer Core	0.5159	0.5300	DC
159-64		0.4584	0.4870	SC
159-65		0.3481	0.3633	DC
159-66		0.1577	0.1561	
159-67	Blanket	0.0944	0.0946	Blanket
158-68		0.0684	0.0668	
159-69		0.0442	0.0435	SS
159-70				
159-71	Reflector			
159-72		0.0252	0.0270	SS
159-73				
159-74				
159-75				
159-76		0.0056	0.0059	SS

[a]Estimated reactor power of 1 watt. Statistical uncertainty 2%. All TLDs are located 76.2 mm behind the reactor interface. The intracell locations are: Core - Columns FG, Blanket and Reflector - Columns HI. The intracell location is specified by dividing the drawers into 16-1/8 in.-wide columns. Each column is assigned a letter with A at the left as one faces the drawer. The TLD spans the columns indicated by the letters.

[b]DC = Double-fuel-column, SC = single-fuel-column, SS = stinless-steel.

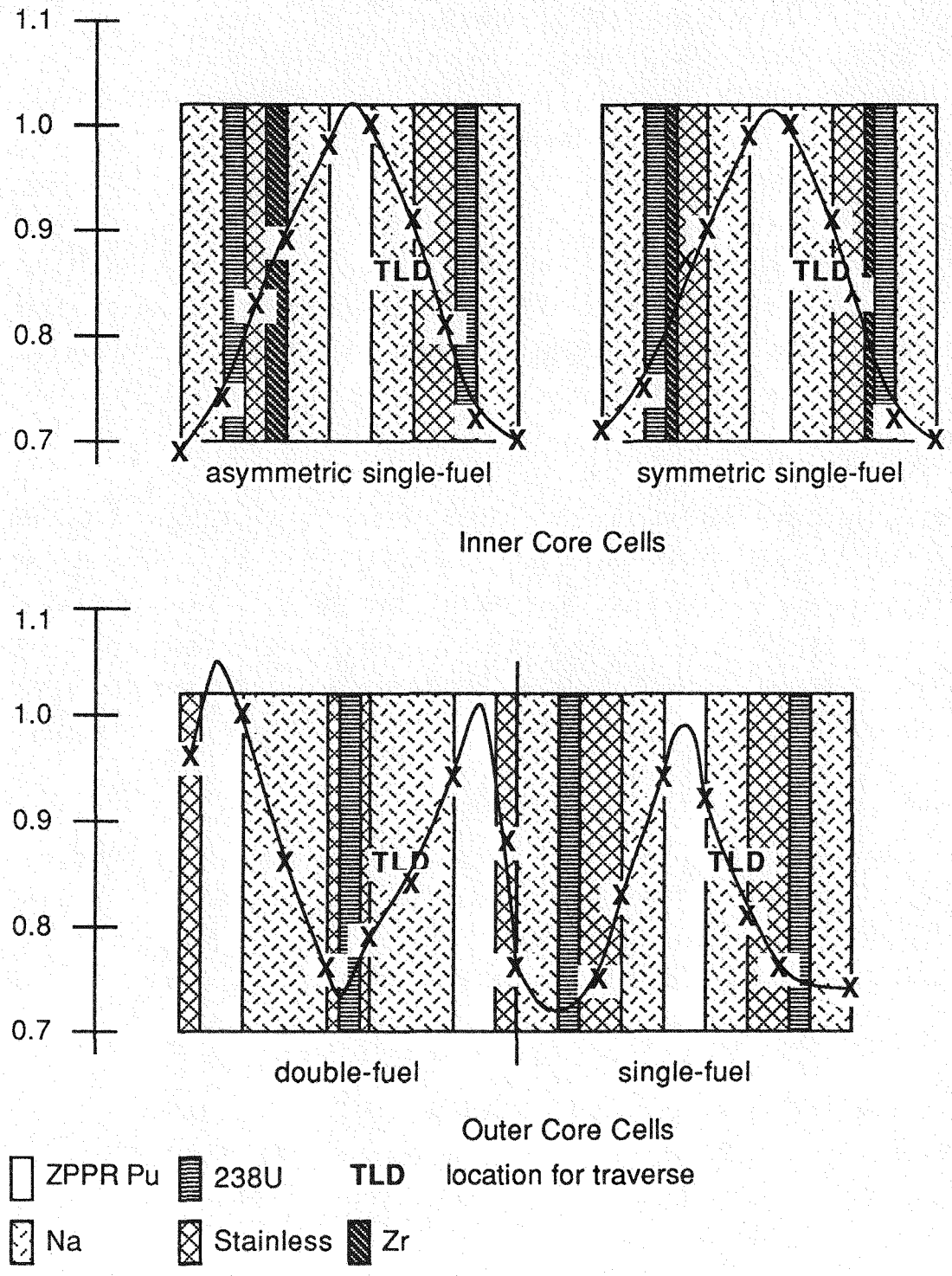

Fig. 10.1 ZPPR 15B Gamma Heating Cell Measurements

11. GAMMA RAY DOSE DISTRIBUTION IN ZPPR-15D (D. N. Olsen and T. S. Huntsman)

The gamma ray dose distribution was measured along the x and y-axes and in the fuel cells of the ZPPR-15D critical reference (ZPR-TM-471, p. 16). Stainless-steel encapsulated ^{7}LiF thermoluminescent dosimeters (TLDs) were irradiated to measure the gamma dose distributions.

Two types of dosimeters were employed in this irradiation. The first was a stainless-steel cylinder of 12.7 mm diameter and 6.4 mm height which can contain up to five TLDs. These dosimeters were loaded into special tunnel sodium plates which replaced normal sodium within the drawer. These dosimeters were used in the core and blanket mapping.

The second type of dosimeter was a stainless-steel cylinder of 3.2 mm diameter and 12.7 mm height which contains one TLD. The dosimeter was sandwiched between the plates of material for the fuel cell measurements.

The irradiation was performed so that the integrated power was about 300 watt-hours. The dosimeters were removed about 20 hours after reactor shutdown.

The TLDs are sensitive to both neutrons and gamma rays. The neutrons contribute approximately 20% of the measured dose. The neutron and gamma contributions can be seperated by calculation of the two fluxes, but the values presented here are for the total dose. The dose rates are given in millirads per second (mrd/s) where 1 rd = 0.01 Gy in SI units.

The dose (neutron and gamma) measured in the xy mapping of the reference is given in Table 11.1. The dosimeters contained two TLDs and the quoted dose rate is the average. The dosimeters were located 76.2 mm behind the half 1 interface. The intracell location is noted in the table and also shown for the fuel drawers as "TLD" in the cell drawings shown in Figs. 11.1 and 11.2.

The dose at the location of the TLD is not the average dose in the cell. The dose distribution in the 15D cells was measured to establish

the relationship between dose at the TLD location and other locations in the cell. This relationship is needed when comparing doses measured in different cell types. The measurements were made in fuel cells located on the y-axis to eliminate the radial gradients across the cell. The TLDs were sandwiched between the plates for the irradiation.

The cell structure measured results are shown in Figs. 11.1 and 11.2. The dose is normalized to 1.0 at the largest experimental value in each cell. Comparison of Figs. 10.1, 11.1 and 11.2 shows the cell structure measured for the 15D fuel cells (uranium fuelled) is more pronounced than for 15B fuel cells (plutonium fuelled). In the single-fuel-column cells, the dose near the fuel plate is as much as 150% higher than at the edge of the cell compared to 40% higher for the single-Pu-column cells. This difference is attributed to greater photon absorption within the Pu fuel plate, which contains about 70% ^{238}U compared to the U fuel plate which contains only about 7% ^{238}U.

Figures 11.1 and 11.2 show that the TLD locations used in the dose rate mapping measurements sample very different portions of the in-cell distribution. This means that one cannot compare directly dose measurements among the different cell types. Variations in measured dose between adjacent cells of different types are obvious for both the inner core and the outer core in Table 11.1. Calculations are needed to relate cell-average dose values to values measured for specific in-cell locations.

TABLE 11.1. Dose Rate (Gamma and Neutrons) in Stainless Steel Encapsulated ^{7}LiF TLDs along the x and y Axis of the Reference Configuration of ZPPR-15D

y-axis		x-axis			
Location Matrix	Dose Rate[a] (mrd/s)	Location Matrix	Dose Rate[a] (mrd/s)	Region	Cell Type[b]
158-48	0.9362	159-48	0.9012		SCS
157-48	0.8970	159-47	0.8750		SCS
156-48	0.9166	159-46	0.8849		SCS
155-48	0.8396	159-45	0.9346		SCS
154-48	0.8438	159-44	0.8879		SCS
153-48	0.8812	159-43	0.9650		SCS
152-48	0.9457	159-42	0.9395	Inner Core	SCS
151-48	1.2120	159-41	1.1490		SDC
150-48	1.1500	159-40	1.1105		SDC
149-48	0.6152	159-39	0.6374		SCA
148-48	0.5387	159-38	0.5851		SCA
147-48	0.5122	159-37	0.5660		SCA
146-48	0.6924	159-36	0.7696		DC
145-48	0.8809	159-35	0.9598		SDC
144-48	0.5391	159-34	0.6101	Outer Core	DC
143-48	0.7459	159-33	0.7167		SDC
142-48	0.4249	159-32	0.4305		DC
141-48	0.1482	159-31	0.1527		
140-48	0.0972	159-30	0.0936	Blanket	Blanket
139-48	0.0664	159-29	0.0690		

[a]Estimated reactor power of 1 watt. Statistical uncertainty 2%. All TLDs are located 7.6 mm behind the reactor interface. The intracell locations are: Blanket - columns HI. The locations in the fuel cells are shown in Figs. 11.1 and 11.2. The intra-cell location is specified by dividing the drawers into 16-1/8 in.-wide columns. Each column is assigned a letter with A at the left as one faces the drawer. The TLD spans the column indicated by the letter.

[b]DC = Double-fuel-column, SDC = Single-fuel-column with 1/8-in. enriched uranium, SCA = Asymmetric single-fuel-column, SCS = Symmetric single-fuel-column.

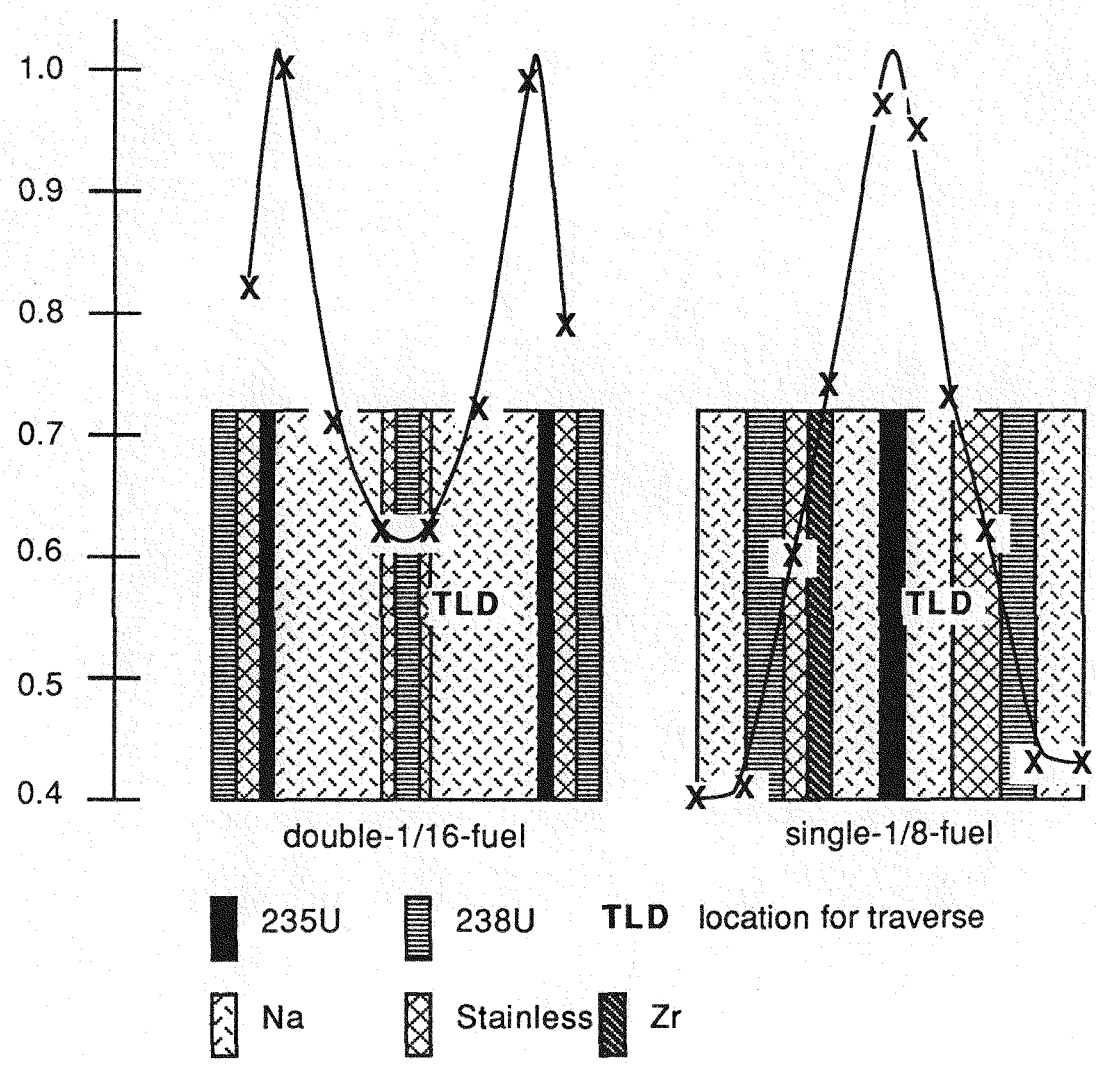

Fig. 11.1 ZPPR15D Gamma Heating Cell Measurements

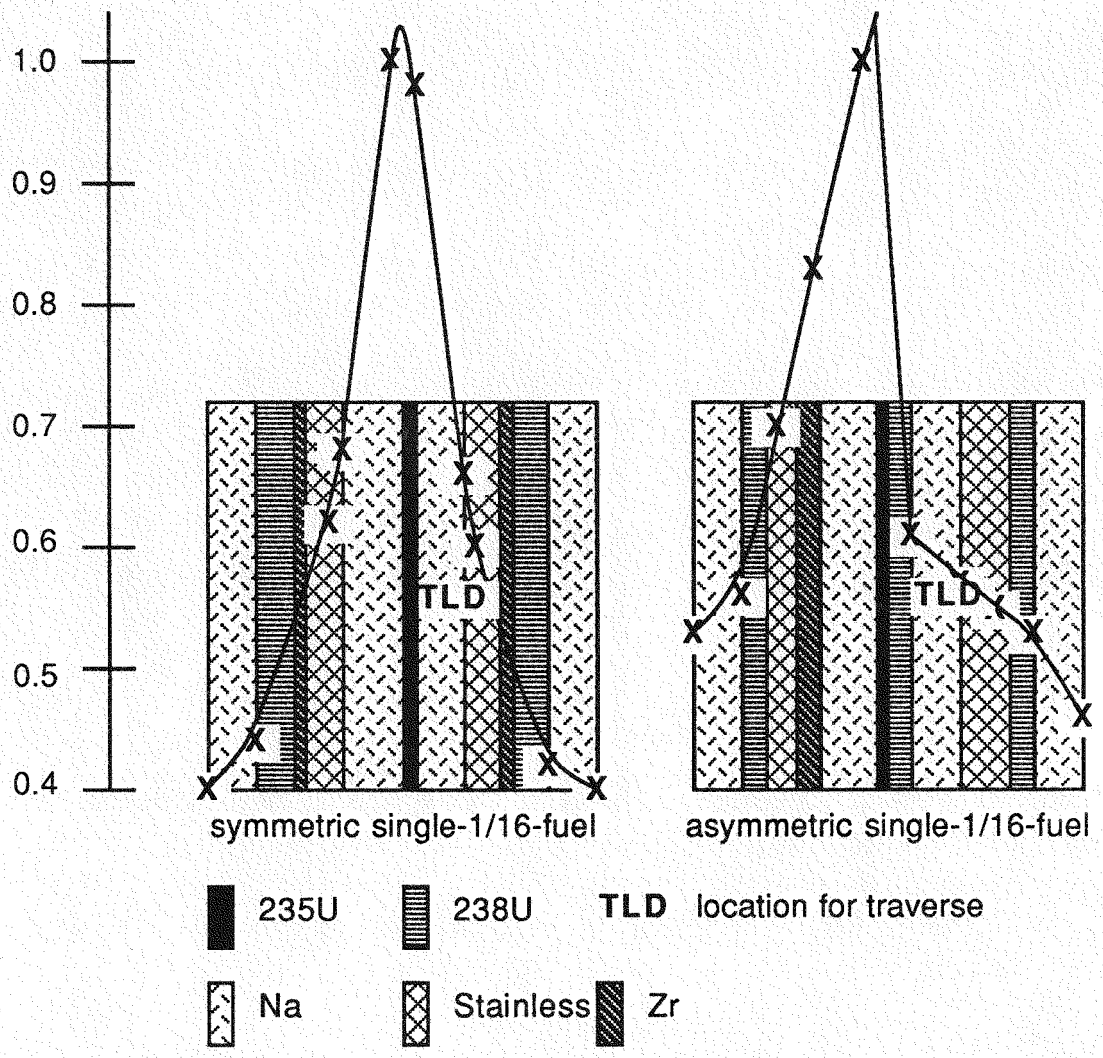

Fig. 11.2 ZPPR15D Gamma Heating Cell Measurements

12. NOISE COHERENCE MEASUREMENTS IN ZPPR-15D (S. G. Carpenter and R. W. Goin)

The short time (millisecond) response of an assembly to a reactivity perturbation can be measured using noise coherence techniques. Spatial decoupling between assembly regions can be investigated by measuring the noise coherence between neutron detectors in the various regions when the assembly is at a constant average power. In a subcritical system, fluctuations about the average power occur as individual fission chains are born and die out. Noise coherence values can also be calculated from the assembly-average kinetics parameters by assuming a point-reactor model. Deviations of measured coherence values from those predicted by the point-reactor model indicate that spatial decoupling is present. A description of noise coherence methods was given for experiments in ZPPR-13 (ZPR-TM-445, p. 35; ANL-RDP-114, p. 3.23).

Measurements in ZPPR-15D used four lithium-glass detectors. The detectors were placed in blanket drawers just outside the core. Two detectors were close together (matrix locations 158-31 and 159-31), a third detector was located 180° away from the closely spaced pair (matrix location 158-66) and a fourth detector was located 90° away from the closely spaced pair (matrix location 141-49). Signals from the detectors were processed by a processed by a fast Fourier analyzer. The coherence function was generated by the analyzer. The frequency range analyzed was 0-10 kHz in increments of 12.5 Hz.

The results from three pairs of detectors along with the detector locations are shown in Figs. 12.1 to 12.3. The solid curves are polynomial least squares fits to the data points. The broken curve represents the coherence obtained for a point reactor model fit. As shown, all detector pairs produce similar coherence values and the calculated response using a point model fits the observed data well. An identical experiment in ZPPR-15A (ZPR-TM-469, p. 140) showed similar results. One difference between the ZPPR-15A and 15D results is the smaller absolute coherence values in 15D. This difference is attributed to the larger value of β_{eff} in 15D (0.006527 vs 0.003357 in 15A). Because

the noise measurements are made with the reactor essentially at delayed critical, the larger β_{eff} value meant that 15D was further from prompt critical which produced shorter prompt fission chains which in turn produced smaller coherence values.

The ZPPR-15D noise measurements were made on May 29, 1986 in reactor run number 319 and in reactor loading number 187.

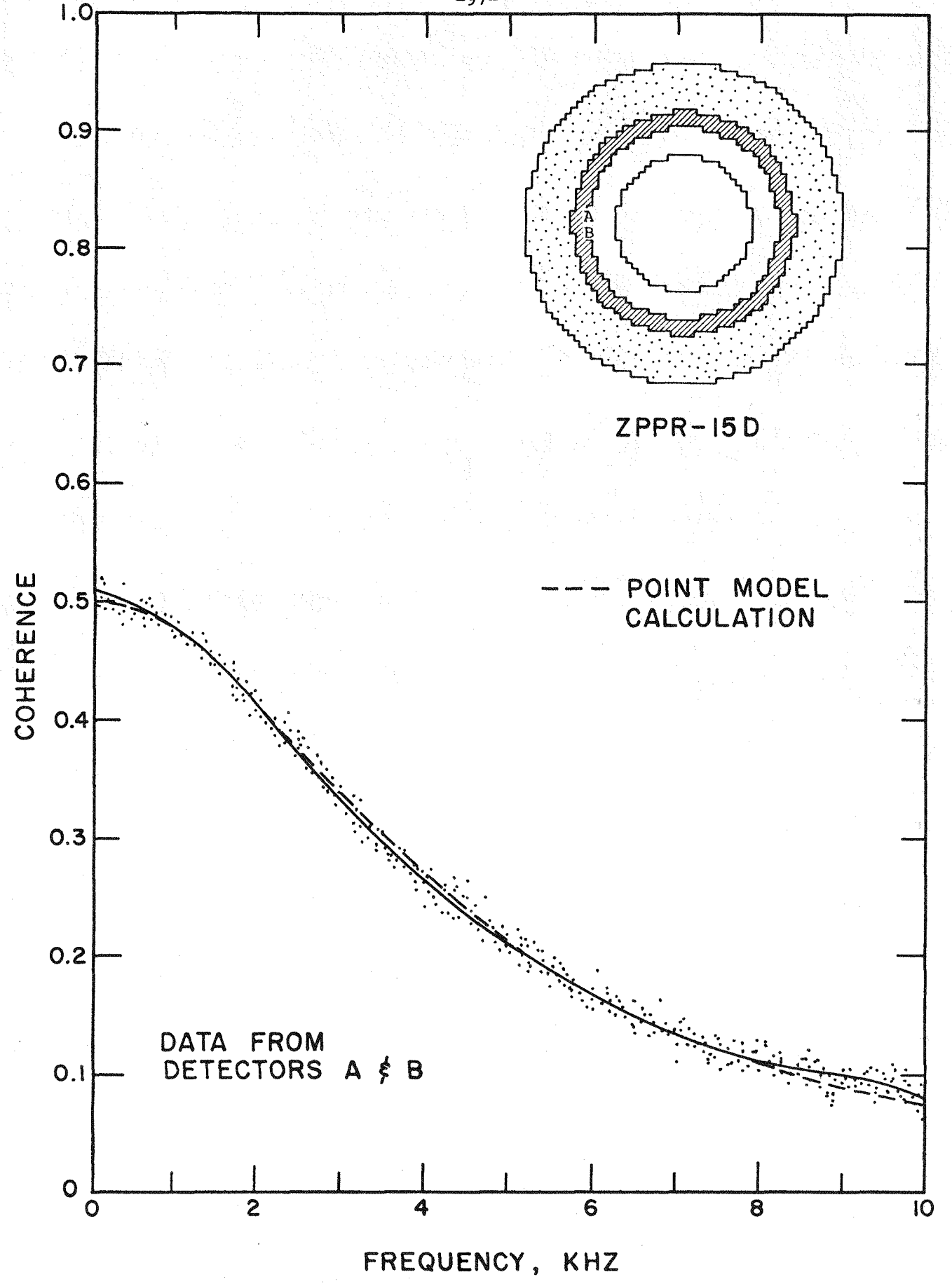

Fig. 12.1. Coherence as a Function of Frequency for Closely Spaced Detectors in ZPPR-15D.

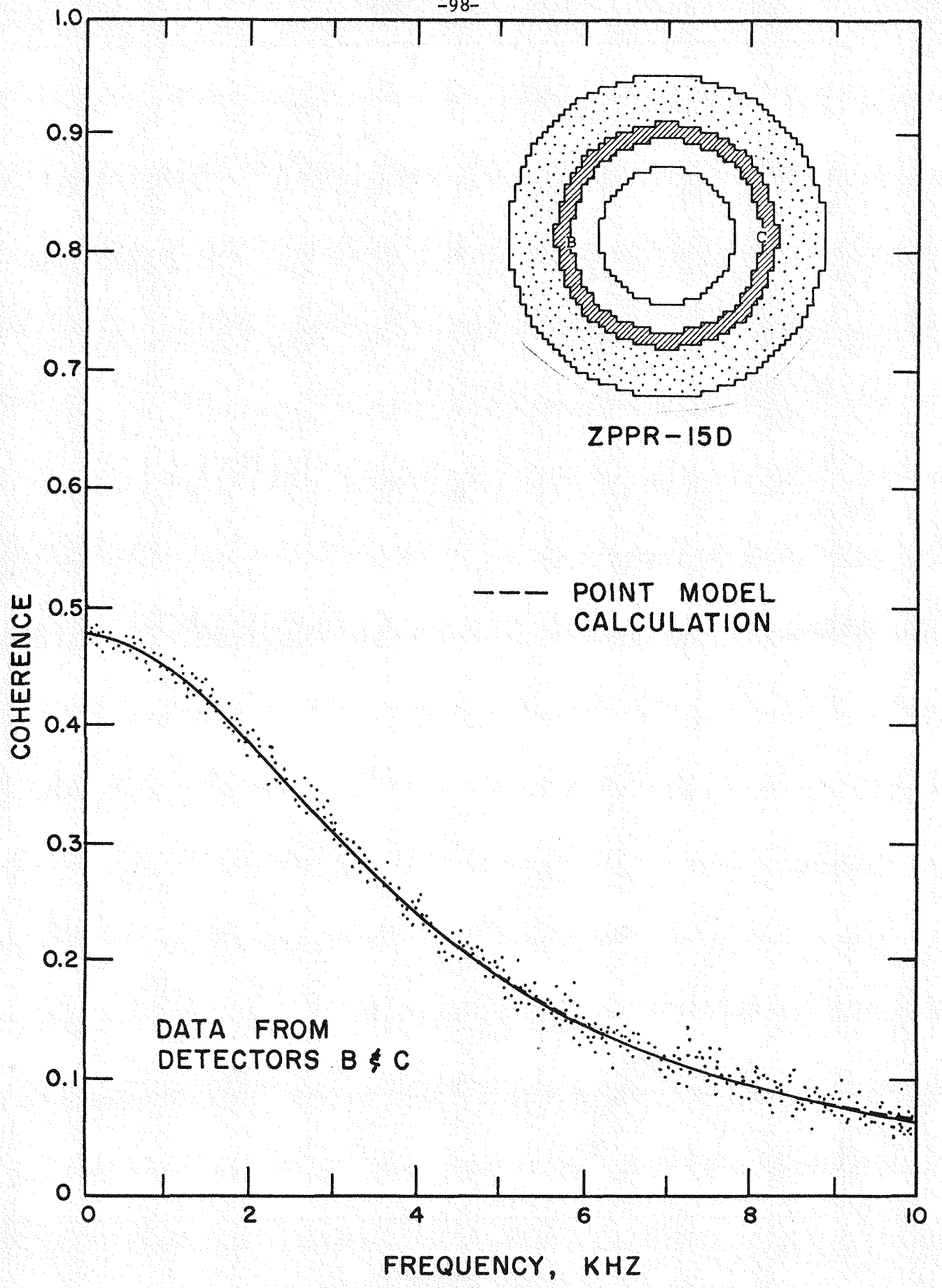

Fig. 12.2. Coherence as a Function of Frequency for Widely Spaced Detectors in ZPPR-15D.

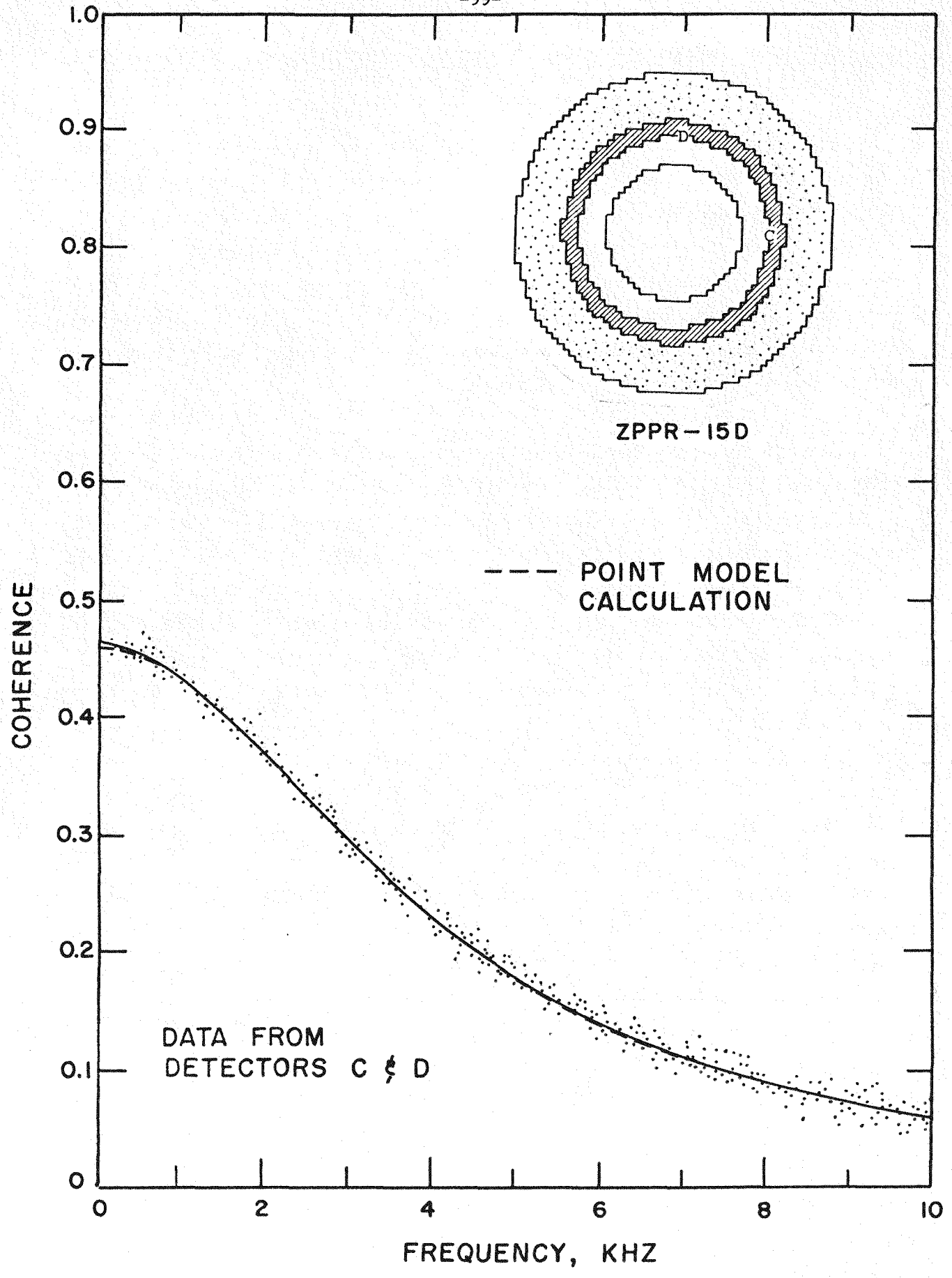

Fig. 12.3. Coherence as a Function of Frequency for Intermediately Spaced Detectors in ZPPR-15D.

13. COMPUTER PROGRAM TO PRODUCE ASSEMBLY DESCRIPTIONS FOR DETERMINISTIC CALCULATIONS (R. W. Schaefer and D. A. Tate)

Assembly descriptions need to be provided as input to computer codes that do assembly eigenvalue and perturbation calculations. The determinstic codes employed at ZPPR to do these calculations get this information in the form of the card image dataset A.NIP3. Until ZPPR-13, reactor models used zone-average compositions so that the volume of input data was quite tractable. Analysis of the decoupled ZPPR-13 cores showed the need to model reactor compositions more accurately, on a drawer-by-drawer basis. This has been the practise since then.

Creation of this dataset has been a long, tedious process, prone to errors because of the volume of data to be handled. Several years ago G. L. Grasseschi wrote a computer program called EZNIP that greatly simplified the process of producing the geometry information. ZPPR loading plans were fed to a preprocessor for EZNIP via computer cards. Drawer compositions were generated by multiple runs of the ADEN (atomic density) code and, although transferred by the computer system, these required extensive editing (changing of isotope names to correspond to those desired on the cross section library). Consequently, this option was ignored by some users.

Now a computer program has been developed that makes generation of the A.NIP3 dataset a quick and simple job. It is standard practice to record geometry and composition information on a computer database when an assembly is being constructed. The idea implemented here is to generate most of the A.NIP3 with a program that accesses this database. This program is called NIPPER.

NIPPER requires a small amount of information not available on the database. This is where the analyst specifies the modeling approximations. The input consists of such things as the portion of the matrix loading encompassed by the model, the region boundaries, and the broad group cross section names that apply to each region.

Drawer masters are the underlying basis for defining regions, materials and compositions. A pure all-master model can be generated. Collections of masters can be lumped into generic types. A specific master or a generic master can be in more than one region to allow for different microscopic cross section names being assigned to the same physical composition.

Two kinds of regions, basic and special are used to define the model. First, basic regions are defined by imposing on the entire model space axial and xy boundaries in a separable fashion (e.g. an axial boundary applied for all xy). This is the way EZNIP operates. Basic region xy boundaries can be defined either in terms of drawer master numbers or in terms of matrix areas. Then special regions can be defined in terms of row and column range and z range, which need not match basic z boundaries. These special regions overwrite space previously defined by one or more basic regions.

Five-character names for regions (A.NIP3 type 06 cards), materials (type 13) and compositions (type 14) are generated by NIPPER according to an easy-to-recognize convention. The first three characters specify the associated drawer master. The fourth character is the basic axial level designator. The first level is A, the second is B and so on. The fifth character is an xy subdivision designator. This is needed for cases where different cross section sets are associated with the same drawer master. For example, 101B1 is the region and composition name for master 101, the second axial level, first occurrence (microscopic cross section type). The corresponding material name is 101BA.

To aid the analyst in using NIPPER to produce an A.NIP3 dataset, the program has three additional capabilities. One is to print a map showing what drawer master is in each matrix position for the requested loading. Another is to compare compositions of different drawer masters, so that the user can decide whether the masters are significantly different. Finally, a nominal input deck for the A.NIP3 generation option can be punched, which the user can then tailor to his needs.

NIPPER is now operational on the Perkin Elmer computer at ZPPR. Most of the capabilities have been debugged. An input description has been written. This program has been used to produce the A.NIP3 dataset for the ZPPR-17A critical reference configuration calculations.